Tome 16 *Août 1978* Numéro 3

うみ

La mer

昭和53年 8月

日仏海洋学会

La Société franco-japonaise d'océanographie
Tokyo, Japon

日 仏 海 洋 学 会

編 集 委 員 会

投 稿 規 定

1. 報文の投稿者は本会会員に限る。
2. 原稿は簡潔にわかりやすく書き，図表を含めて印刷ページで**12**ページ以内を原則とする。原稿（正**1**通，副**1**通）は，（〒101）東京都千代田神田駿河台2-3　日仏会館内　日仏海洋学会編集委員会宛に送ること。
3. 編集委員会は，事情により原稿の字句の加除訂正を行うことがある。
4. 論文（欧文，和文とも）には必ず約200語の欧文（原則として仏文）の要旨をつけること。欧文論文には欧文の要旨のほかに必ず約500字の和文の要旨をつけること。
5. 図及び表は必要なもののみに限る。図はそのまま版下になるように縮尺を考慮して鮮明に黒インクで書き，論文の図及び表には必ず英文（又は仏文）の説明をつけること。
6. 初校は原則として著者が行う。
7. 報文には1編につき50部の別刷を無料で著者に進呈する。これ以上の部数に対しては，実費（送料を含む）を著者が負担する。

RECOMMANDATIONS A L'USAGE DES AUTEURS

1. Les auteurs doivent être des Membres de la Société franco-japonaise d'océanographie.
2. Les notes ne peuvent dépasser douze pages. Les manuscrits à deux exemplaires, dactylographiés sur papier fort, doivent être envoyés au Comité de rédaction de la Société franco-japonaise d'océanographie, c/o Maison franco-japonaise, 2-3, Kanda Surugadai, Chiyoda-ku, Tokyo, 101 Japon.
3. Le Comité de rédaction se réserve le droit d'apporter, le cas échéant, des modifications mineuses aux manuscrits ainsi que de demander aux auteurs de les corriger.
4. Des résumés en langue japonaise ou langue française sont obligatoires.
5. Les figures au trait seront tracées à l'encre de Chine noire sur papier blanc ou sur calque. Les légendes des figures et des tableaux sont indispensables.
6. Les premières épreuves seront corrigées, en principe, par les auteurs.
7. Un tirage à part des articles en cinquante exemplaires est offert gratuitement aux auteurs. Ceux qui en désirent un plus grand nombre peuvent les faire établir à leurs frais.

La mer (Bulletin de la Société franco-japonaise d'océanographie)
Tome 16, N° 3, pp. 111 à 123, Août 1978

Origin of Trenches*

Michihei HOSHINO**

Abstract: The author maintained that the oceanic trench was formed as a furrow left behind when the ocean floor upheaved. The depths of two guyots which are located about 500 km apart on the Japan Trench are almost the same, and Middle Cretaceous shallow marine fossils were collected from the top of both guyots. The author urged that this phenomenon impresses the immovability of trench floor. The cause of origin of the trench is an upheaval of the ocean floor as a result of material rising from the upper mantle.

1. Introduction

In a previous work (HOSHINO, 1962) the author argued the case for a marked rising of sea level by the expansion of the earth, especially by the upheaving of the ocean floor, and he explained the formation of submarine canyons as a result of this uprising of sea-level. Later he maintained (HOSHINO, 1970) that the oceanic trench was formed as a furrow left behind when the ocean floor upheaved. After that he published a book entitled "Eustacy in relation to orogenic stage" (HOSHINO, 1975) in which he explained the remarkable uprising of sea-level after the Late Miocene, and also he referred to some related problems—submarine canyons, coral reefs, coastal plains, landbridges and so on—. The term "orogenic stage" was used to mean the stage of great mountain building and not the stage of folding. He thinks that the great mountains were formed by block movement (so-called epirogenic movement) in the Anthropogene (Pliocene-Recent) and the Triassic period (HOSHINO, 1978).

Recently, the author attempted a survey to prove the immovability of the trench floor. At the boundary between the Kurile-Kamchatka Trench and Japan Trench, there is the Erimo Seamount. This seamount is a guyot rising from the trench floor at 7,500 m to about 4,000 m. Middle Cretaceous shallow fossils were collected from the top of the Erimo Seamount (TSUCHI and KAGAMI, 1967). The Daiichi Kashima Seamount is located at the boundary between the Japan Trench and the Izu-Bonin Trench, and it has the same depth as the Erimo Seamount. If the trench floor is an immovable region then it should be possible to collect Middle Cretaceous shallow marine fossils from the top of the Daiichi Kashima Seamount. He tried a survey with this in mind, and did indeed find the same types of fossils as those of the Erimo Seamount on the top of the Daiichi Kashima Seamount (The Daiichi Kashima Seamount Res. Group, 1976). In the world, there are many other pieces of evidence that show −4,000 m Middle Cretaceous sea-level. As a consequence of this survey, he believes that the idea of the immovability of the trench floor has received important support, but there are few geologists who agree with this hypothesis.

There are those who accept the idea of earth expansion, but they urge a large scale expansion of the earth as a cause of continental drift. The author cannot support a large scale expansion of the earth, and he cannot understand their hypotheses to permit the depression of trenches. Absolute depression of the earth's crust means shrinkage of the earth. Any hypothesis for the origin of oceanic trenches may be a touchstone for all hypotheses on crustal dynamics.

2. Relation between the orogenic belts and distribution of trenches

Major recent trenches are distributed at the magin of the Pacific, but very rare in the

* Received May 29, 1978
** Faculty of Marine Science and Technology, Tokai University, Shimizu, 424 Japan

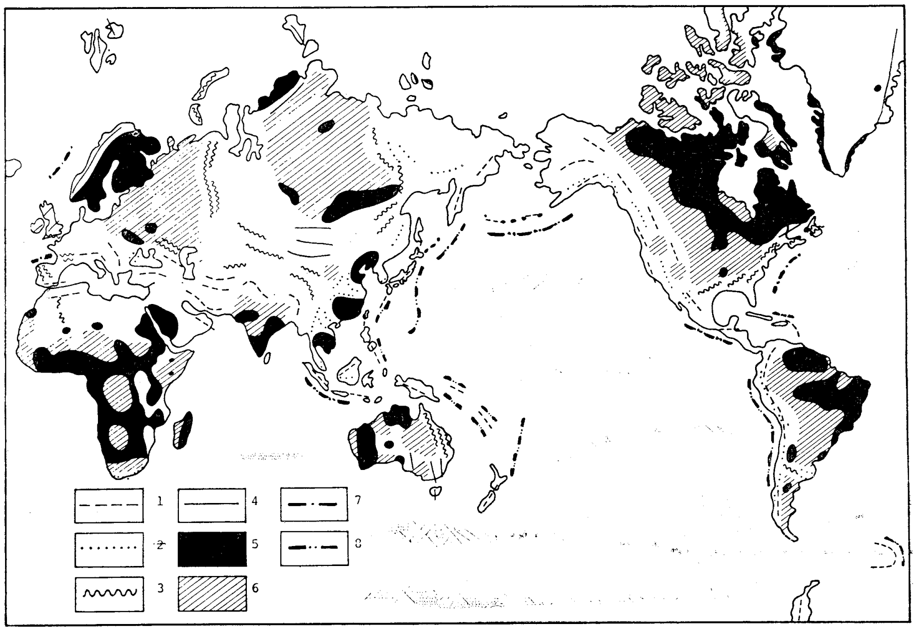

Fig. 1. Distribution of orogenic belts and Precambrian crust of the world. 1; Cenozoic orogenic belts, 2; Mesozoic orogenic belts (1 and 2, the Alpine orogenic belts), 3; the Hercynian orogenic belts, 4; the Caledonian orogenic belts, 5; exposed Precambrian rocks, 6; covered Precambrian rocks, 7; fossil trenches (Caledonian and Hercyian), 8; resent trenches.

Atlantic and Indian Oceans. Judged from the viewpoint of orogenic belts, the distribution of recent trenches coincides with the Alpine orogenic belt except Tethyan region. Are there any relationships between Caledonian or Hercynian orogenic belts and the distribution of trenches ? Off the western coast of Scandinavia which corresponds to the region of the Norwegian Sea, there is sedimentary basin with wedge sediments (TALWANI and ELDHOLM, 1973). As the basement of this basin is oceanic crust, the depression may be called a "fossil trench". The P wave velocity of the lowest part of the sediment is 4.4 km/sec, and Talwani and Eldholm described that this velocity shows the upper Palaeozoic formations. They also said that this depression extends to the North Sea, and the geologic age of the lowest sediments of the North Sea is of the Devonian period. So it may be concluded that the formation of this depression was related to the Caledonian orogeny. A similar depression under the continental rise is reported from the neighboring Barents Sea (RENARD and MASCLE, 1975). Perhaps, a similar depression may be observed from all the regions off Caledonian orogenic belts. Crustal movements of such an area is characterised by the so-called epirogenic movements—vertical block movements with faulting (TALWANI and ELDHOLM, 1973).

A typical Hercynian orogenic belt is seen in the Appalachia Mountains of the eastern part of the United States, and off the eastern coast of the United States there is a famous depression with a thick wedge sediments (HEEZEN, 1962). Recently, SHERIDAN (1975) described the sediment filling this depression and the geologic age of the oldest sediments is Triassic. He urged that formation of this depression is related to the opening of the North Atlantic. However, characteristic so-called epirogenic crustal movement in the Triassic period is not limited to the area around the North Atlantic: we can observe the same in many regions of the world. The author argued that this crustal movement in the Early Triassic is not related to continental drift, but is related to the expansion of the earth (HOSHINO, 1978). In

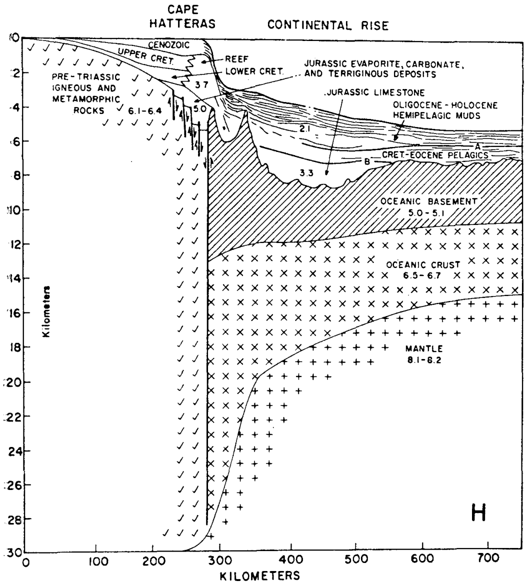

Fig. 2. Diagrammatic structural cross section of the Cape Hatteras continental margin (from SHERIDAN, 1975).

Europe, one of the Hercynian orogenic belts is distributed on the northern part of the Iberian Peninsula. Under the outer continental margin of this region there is a depression which has been filled with sediments since Triassic times, and is described as the "fossil North Spanish trough" (RENARD and MASCLE, 1975). The eastern continental margin of the Atlantic show similar conditions as those of western margin.

As mentioned above, all orogenic belts of Phanerozoic time are associated with filled trenches. The cause of this phenomenon is related to the crustal development of the earth. The orogenic belts of Criptozoic time are distributed in the continents, but the orogenic belts of the Phanerozonic time are distributed on that part of the continent which borders the ocean.

There is no trench (filled or unfilled) off the shield regions of the world. However in this case, the basement of oceanic crust gradually changes upward from continental margin to ocean (SIESSER *et al.*, 1975). There is no trench at some marginal parts of the Pacific, e.g., the region between the Izu-Bonin Trench and the Mariana Trench and off California coast. Though MENARD (1964) stated that the Izu-Bonin and Mariana Trenches are separated from each other by volcanoes, separation of the two trenches is actually due to a non-volcanic submarine plateau. The author (1969) maintained the Yamato Bank in the Japan Sea, the Daito Ridge in the northwestern corner of the Philippine Sea and the Ogasawara Plateau which is located between the Izu-Bonin Trench and Mariana Trench may be formed of Precambrian basement from the evidence of the ultra deep earthquakes. Already a Precambrian rock specimen has been collected from the Yamato Bank (HOSHINO and HONMA, 1966), and acidic plutonic and metamorphic rocks were collected from the Daito Ridge (MIZUNO *et al.*, 1975). Paherps older continental rocks may be sampled from the Ogasawara Plateau in future.

It is well known that there is no trench off California, and it is explained that this due to the extension of the continent (GUTENBERG and RICHTER, 1954). The existence of Precambrian rocks was reported by EMERY (1960) from an island which exists in the continental borderland off southern California. According to DUNBAR and WAAGE (1969, Fig. 7-18), the sedimentary basin of the Late Precambrian Belt series can be extended to the sea bottom off southern California. MAXWELL (1975) described that the sedimentary materials of the Belt series was not transported from a western region, but since the sedimentary basin of the Belt series extends under the sea, it is not possible to determine a lost continent from the subaerial Belt series. We must remember that the Precambrian orogenic belts are distributed only inside the continents. According to these evidences the author considers that the fact of no trench off California may be related to the distribution of the Precambrian basement.

3. Geologic and geophysical characters of the trench

A. Topographical characters of the trench

One of the topographical features of trenches is the uniformity of the depth. With respect to this problem, MENARD (1964) referred that the uniformity of the depth of main trenches of the Pacific shows the limit of the crustal downwarping, and von HUENE (1975) described that the uniformity of depth and topography of trenches of the Pacific reflects a similar origin for trenches. The uniformity of the depth of the trench is not only related to the recent trenches, but also related to the fossil trenches. For instance, the depth of the basement of the fossil trench under the continental rise off the eastern coast of the United States is about 10 km, and the depth of the basement of the fossil trench off Nova Scotia is also the same (SHERIDAN, 1975). Perhaps a similar circumstance may be exist in the Hawaiian Trench because the depth of the Mohorovicic discontinuity is 11.5–13 km (FURUMOTO *et al.*, 1968). Although, the topography of the Southwest Japan Trench is obscure, and its depth is only 4–5 km, thickness of the sediments being 6.5 km (MURAUCHI *et al.*, 1968), the depth of the basement of this trench is equal to the others.

MENARD (1964) suggested that the depth of the trench is not so important, rather the relative depth between the ocean floor and the trench is important as the measure of the crustal depression. The author maintains that the uniformity of the trench depth is the most essential character of the trench, though the relative depth is also important as it shows the magnitude of upheaving of the ocean floor.

Regarding the uniformity of the depth of trenches, it is very interesting to consider the depth of a guyot which is located on the about 500 km apart on the Japan Trench are almost the same, and Middle Cretaceous shallow marine fossils were collected from the top of both guyots. The author urged that this phenomenon impress the immovability of trench floor.

The second character of the trench topography is the marginal swell. The marginal swell, with an elevation of 200–300 m and the width of 200–300 km is located on the boundary between the oceanward slope of trench and the ocean floor. In many cases volcanoes are distributed on the marginal swell, for exsample low hills and volcanoes are distributed on the marginal swells off the Aleutian, Kurile and Middle America Trenches (MENARD, 1964). It is difficult to explain the origin of the swell as a result of compressional force since volcanoes are distributed on the marginal swell. Volcanoes occur only in the field of tension (TANNER, 1973), and de SITTER (1956) and UDINTSEV (1967) considered that the mantle materials are uprising here.

The third character of trench topography is the "ridge and depression" on the oceanward slope of the trench. In the case of the Aleutian Trench, valleys of several kilometers in width and 50 km in length are developed by normal faulting; the ridges are fault blocks and the valleys are fault zones (HERSEY, 1961). Similar topography in the Japan Trench was called a "long narrow depression" (IWABUCHI, 1968). Both the marginal swell and the ridge and depression are not formed by compressional force.

B. Trench sediments

Generally, sediments of a trench are thin, and there are many parts which have no sediment. However, a trench which has no sediment is located along the island arc, other trenches which have large rivers in their hinterland have a plentiful supply of sediments and the trench topography is obscured. It is known that the volume of trench sediments is related to the age of trench formation and its palaeoenvironment.

According to the plate tectonic concept, the oceanward slope of a trench should be covered by pelagic sediments, but in many places, pillow lavas and basalt flows are distributed on the ocean side slope of the trench (FISHER, 1975). Though there are thick sediments on the neighbouring ocean floor, there is little sediment in the New Hebrides and Vityaz Trenches. This makes it difficult to postulate plate sinking here (HAYES and EWING, 1971).

Since SCHOLL *et al.* (1968) pointed out that the sediments of the Peru-Chile Trench are not deformed, many geologists considered this problem and they have discussed non-deformed trench sediments. OLIVER (1970) suggested that the trench sediments are not deformed because they are too soft to be deformed by compressional force. However, since the uppermost sedimentary layer of the Japan Trench is cut by fault (LUDWIG *et al.*, 1966), the author cannot agree the idea that trench sediment is too soft to be deformed. We observed slightly deformed sedimentary layers in the air-gun records of the Southwest Japan Trench. We have also observed an abyssal hill in this trench and an intrusive body (HOSHINO, 1964). According to this phenomenon the author considers that the deformation of the trench sediments is caused by igneous diapiric activity. Deformation of fossil trench sediments off eastern coast of North America is also caused by the diapiric intrusion (SHRIDAN, 1975). At present, the problem of the deformation of sediment on the lower landward slope of trenches is under discussion. CHASE and BUNCE (1969) maintained that subduction of the plate is proved by the deformed sedimentary layer on the seismic profiler records at the boundary between the slope and ocean floor off Barbados Island. However, as GROW (1973) pointed out, these records cannot deny the possibility that the deformed sediments are the product of slumping.

During the deep-sea drilling by the Glomar Challenger on the lower landward slope of the Southwest Japan Trench (Site 298), deformed young sediment was obtained, and many plate tectonists urged that this phenomenon was caused by subduction of the plate. Coring length of this site is 611 m, and upper 194 m is not deformed. The shipboard geologists described all core sample belongs to the Quaternary system. The author has some doubts about the age determination by microfossils and is inclined to judge the age of the boundary between deformed and nondeformed sediment to be the Early/Middle Pleistocene, namely the Rokko movement stage of the western Honshu which is at the same orogenic stage as the Pasadenian in California (HOSHINO, 1975). Crustal movement of the Pasadenian stage is observed in many places of the world (HOSHINO, 1975). After this stage, remarkable crustal movement is not observed on land, and "terrace stage" or real glacial stage had been commenced. Also at Site 181, the landward slope of the Aleutian Trench, the upper 170 m of sediments is not deformed (SEELY *et al.*, 1975). The author considers that the conclusion that the sediment on the landward slope of a trench was deformed because of the sinking of the plate, must be reexamined.

The wedge sediments of the Aleutian and Washington-Oregon Trenches (e.g., Site 174 of the G. Challenger) are horizontal deltaic sediments of the Middle to Late Pleistocene time (SCHOLL, 1975). The thickness of this wedge sediments increases toward land, and at the lower part of the slope the thickness of the wedge is 1–1.5 km. It is most significant that the geologic age of the wedge sediments is post Early to Middle Pleistocene. Namely the age of trench formation accords with the Pasadenian stage which is the latest "epirogenic" block movement stage of Earth's history (HOSHINO, 1978). As the fossil trench off the eastern coast of the United States had been formed in the Early Triassic "epirogenic" stage, it is beyond doubt that the formation of the Washington-Oregon Trench is in the Anthropogene epirogenic stage. Geologic phenomena related to the Triassic and Anthropogene epirogenic stage had been described in other paper (HOSHINO, 1978). According to the data of the Washington-Oregone Trench (SCHOLL, 1975), the depression which has a 1–1.5 km relative depth was formed at the boundary between ocean floor and continental slope. The author (1975) urged that sea-level rose 1,000 m in this time as the result of ocean floor upheaving.

In many cases, recent trench sediments are not composed of pelagic red clay; for instance, the sediments of the Japan Trench is composed of blue mud which contain much organic material (HOSHINO, 1962) and this material is the basic food for trench animals. Biologist have discussed the antiquity of the trench fauna (ZENKEVICH and BRISTEIN, 1960; MENZIES *et al.*, 1961), but it seems to me that they refrained from giving any definite opinion on the problem. BELYAEV (1971) suggests that the development of the trench fauna is very rapid, and implies that the age of the formation of recent trench is the Cenozioc era. Relatives of the trench fauna inhabit the landward slope, and did not inhabit on the ocean floor. On the contrary, the pelagic red clay fauna is a descendant of the continental margin fauna (MENZIES *et al.*, 1973).

C. Gravity anomalies and terrestrial heat flows around the trenches

From the initial stage of maritime gravity observations, the problem of negative anomaly associated with oceanic trenches had been discussed by many earth scientists. Based upon this anomaly, the concept of backling theory was proposed as the origin of trenches (VENING MEINESZ, 1948). The author, urged that the negative gravity anomaly zone along the lower continental slope reflects the thick Neogene sedimentary basin at the base of continental slope (HOSHINO, 1969). The same conclusion was reached by HAYES and EWING (1971), and it is impossible to relate this gravity anomaly with the origin of trench.

In many places on the marginal swell, a positive gravity anomaly was observed. For exsample, on the marginal swell of the Kurile-Kamchatka Trench, gravity anomaly of $+50\sim60$ mgal was recorded (WATTS *et al.*, 1976). They suggested that this value does not agree with the plate theory. VENING MEINESZ (1948) considered that this positive anomaly indicates compensating uprising mantle materials which occur at the boundary of the tectogene. Though UYEDA (1975) and SEGAWA and TOMODA (1976) urged that this phenomenon is related to the stress system with the convergence of the lithosphere, it is impossible to suppose such a stress system from the geological and geophyisical character of the marginal swell. A positive gravity anomally was observed on the Hawaiian marginal swell, too (WATTS *et al.*, 1976). The most reasonable explanation is to suppose the uprising of heavy materials from the upper mantle.

Plate tectonists maintain that the trench is the part of sinking of the plate, and the value of terrestrial heat flow is lower than in other parts of the earth. Indeed the value of terrestrial heat flow from the trench floor is generally lower than that from the island arc or ocean floor, but frequently a slightly higher value is observed from the marginal swell. Namely, the curve of the heat flow value coincides with the topographic profile. It is highest at the island arc, lowest at the trench floor, and slightly higher at the marginal swell than on the ocean floor (YASUI *et al.*, 1970). At the marginal swell of the Ryukyu Trench,

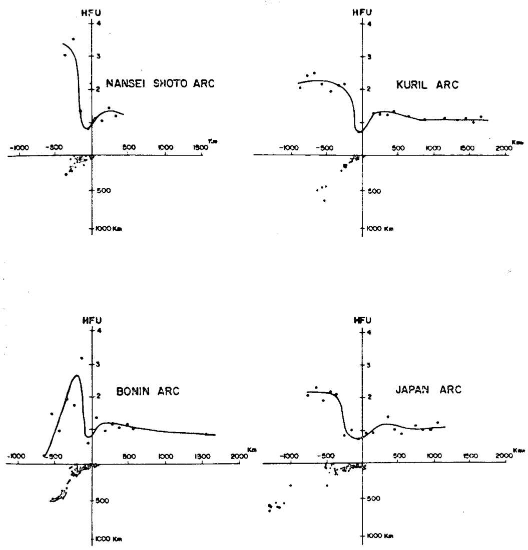

Fig. 3. Profile of heat flow, averaged at 100 bm intervals from the trench axis (from YASUI *et al.*, 1970).

three high isolated heat flow positions (2.46, 4.20, 2.40 HFU) were detected (WATANABE *et al.*, 1970). They described that this high values had not been observed at the eastern part of the Kurile, Japan and Mariana Trenches, and any explanation cannot resolve this phenomenon. But it is well known that high heat flow volues have been observed in the neighborhood of the Southwest Japan Trench of the northern part of the Shikoku basin. Though these high values are explained as related to the Izu-Bonin Ridge, the parts of highest heat flow are not so close to the ridge, but are observed from the ocean floor.

Deep oceanic trenches are characteristic topography of the Pacific, and the heat flow value of the Pacific (mean value is 1.7 HFU) is higher than from the Atlantic and Indian Oceans (LANGSETH and von HERZEN, 1970). They suggested that the high heat flow of the Pacific reflects the youthfulness of the Pacific. The author considers this fact to be related to the origin of the Pacific trench.

D. Earthquakes and trenches

For many years the concept of a seismic plane has been established and many earth scientists are interested in the relationship between trench and earthquakes. The seismic plane is called

Benioff zone, and BENIOFF (1949) maintained that this seismic plane is a reverse fault plane or a thrust plane. A distinct seismic plane cannot be observed in some trench regions. BELOUSSOV (1971) described that among many geological and geophysical phenomena, only the earthquake mechanism shows that trenches are place of compression. However, recently, the records of the earthquakes of tensional (normal fault) origin have been collected. KANAMORI (1972) reported the great earthquakes of normal fault origin occurred under the Japan and Aleutian Trenches, and KATSUMATA and SYKES (1969) reported that earthquakes which occurred on the marginal belt of the Philippine Sea have a reverse fault origin, but TANNER (1973) stated that many earthquakes have a normal fault origin. According to these data we know that the trench region is not a simple compressional field. KANAMORI (1972) urged that normal fault under the trench occur as a result of tearing off of the cool plate. The author cannot agree with his opinion based on the data of heat flow and gravity observation at the marginal swell.

Deeping of the earthquake foci from trench to continent, cannot be observed in some trenches. Around the Greater Antille Islands, the earthquake foci deepen from the Puerto Rich Trench toward the south, and from the Muertos Trench toward the north (SYKES and EWING, 1965), consequently the profile of distribution of foci shows a V form. These distributions of earthquake foci are not only observed at an island arc-trench system region, but also is observed in the Hindu Kush Mountains (HIRAYAMA and ASANO, 1972). HATHERTON (1975) discribed that the relation between the inclination of the Benioff zone and shallow earthquakes which occurred in an active margin is obscure. The author (1969) considered that there are no relation between shallow earthquake and trench, because shallow earthquakes are related to the Neogene sedimentary basins on the "active" continental slope. The earthquakes which are located in the Benioff zone are due to continental massif and ocean relationship.

4. Origin of trenches

Scince early in the Twentieth Century, many geologists have discussed the origin of trenches. For instance, SUESS (1906) asserted the origin of trench as down folding as a result of earth's shrinkage. Nowadays nobody believes in the concept of a shrinking earth. Though geologists of Netherland tried to explain the origin of trench by the concept of buckling crust (VENING MEINETZ, 1930; KUENEN, 1936; UMGROVE, 1947), the sediments of many trenches are not so thick, and negative gravity anomaly observed on the landward slope of a trench is not related to the buckling materials. VAN BEMMELEN (1954) urged that the upheaving of the island arc was caused by granite that was differentiated from basaltic magma. Basaltic magma moves from the ocean side to the lower island arc to compensate for uprising granite magma, then a trench was formed at the base of the continental slope. But as the author has stated elsewhere (HOSHINO, 1975), the upheaving of the island arc in the Anthropogene period was caused by basic materials from the upper mantle.

Plate tectonists maintain that the formation of a trench is related to sinking of the plate, but the nature of the plate is very obscure and it is very difficult to understand the idea of a pair of upwelling and desending plates.

The hypothesis of the author on the origin

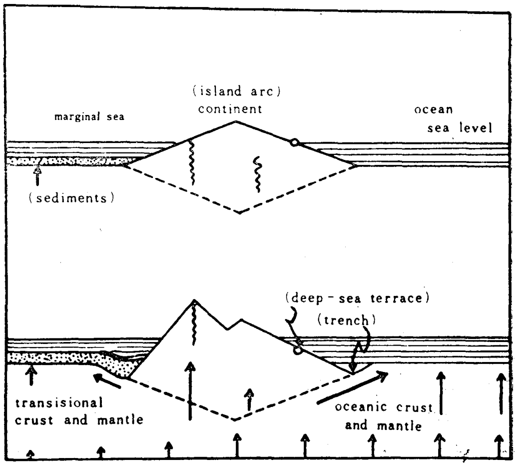

Fig. 4. Explanatory scheme for the origin of trenches (from HOSHINO, 1970)

of trenches was described in a other paper and a book (HOSHINO, 1970: 1975). After that, he obtained considerable evidence from the survey of the Daiichi Kashima Seamount where a guyot is located on the trench (The Daiichi Kashima Seamount Res. Group, 1976). Recently, the author obtained same evidence from the J-anomaly Ridge in the northeastern corner of the fossil trench off the eastern coast of the United States (The Shipboard Scientific Party, 1975). The idea of the author is based on the 'insignificant' expansion of the earth. In his meaning, the expansion of the earth means the upheaving of the ocean floor caused by differentiation of the upper mantle materials, and that part left behind is the valley which is called a trench.

The fact that there is no trench around the Precambrian shield region, the distribution of the Caledonian and Hercynian fossil trenches around the Norwegian Sea and the North Atlantic and recent trenches around the Pacific Ocean, all show that the upheaving of the Pacific Ocean floor took place in the latest stage of the earth's development. WORZEL (1975) described that the P wave of the lower crust and the upper mantle of the Pacific Ocean is much more basic than in the other oceans. LANGSETH and von HERZEN (1970) described that the heat flow of the Pacific Ocean is higher than that of the Atlantic and Indian Ocean, and this evidence implies the youthfulness of the Pacific Ocean. From the view point of the earth's development, the Cryptozoic is an acidic igneous stage (continental stage), and the Phanerozoic is a basic volcanic stage (oceanic stage). These kinds of evidence, namely the lower crust and upper mantle of the Pacific Ocean is younger than the Atlantic and Indian Oceans, show that the activity of the Pacific is the youngest of the earth's development.

From the view point of the plate tectonics hypothesis, the fracture zone off the coast of California has a special character, but following the author's hypothesis these ridges are the boundary of the differential vertical movement of the crust. The depth of the northern floor of the Mendocino Fracture zone is less than the southern floor, and the terrestrial heat flow of the nothern floor is higher than to the south (MENARD, 1964). In this case, the thinness of oceanic crust of the northern region is caused by the existence of a 7 km/sec layer which belongs to the mantle, and the smallness of the depth of this region is caused by the upheaving of the basement of the oceanic crust. These phenomena show the original form of the expansion of ocean floor, and MENARD (1964) described that the upheaving of the ocean floor as a result of the decrease of P wave velocity by 0.8 km/sec due to decrease in density of mantle material. The author seconds his opinion. The author cannot agree with the opinion of BELOUSSOV (1971) or SHERIDAN (1975) that 7 km/sec layer is produced as a result of mixing of the continental crust and upper mantle materials. With regard to the formation of trenches, the upheaving ocean floor of the northern part of the Mendocino Fracture Zone produced the Washington-Oregon Trench in the Anthropogene period, and the non-upheaving of southern floor is related to the non-production of an oceanic trench. The Venezuela basin of the Caribbean Sea has the Muertos Trench in the northern part, the Los Rogues Trench in the southern part and the Grenada Trough in the eastern part, and the central part of the basin is gradually domed up with relative height in 700-800 m from the margin of the basin (OFFICER *et al.*, 1957; EWING *et al.*, 1971). The author considers that the origin of the depression around the Venezuela basin may be the same as that of the typical oceanic trenches around the Pacific Ocean.

Many geologists have pointed out that the trench is not a compressional field since the layering of trench sediments is not deformed. Slumping sediments or deformed sediments occur on the landward slope of the trench. It is not sufficiently proved that the slumping or deformation of sediments was due to the subduction of the plate. On the contrary, the deformation of the young sediments on the landward slope of the Southwest Japan Trench and Aleutian Trenches occur some 100 m-200 m under the sea-bottom, thus showing that the deformation of sediments occurred at the time of worldwide crustal disturbance. In short, it was produced by the Pasadenian orogeny in the Early/Middle Pleistocene.

The fact that there is a fossil trench which was filled by the sediments since the Triassic period under the continental rise and that the recent trenches have sediments since the Early Anthropogene, shows that the mechanism of the formation of trenches is upheaving of the ocean floor which was caused by a large scale uprising of mantle materials. This event was called "volcanic orogeny" by the author (HOSHINO, 1978). If the trench is a furrow left behind when the ocean floor upheaved, the trench floor show primary surface of the earth, and the uniformity of the trench depth shows the surface of the spheroidal primary earth.

As to the origin of the Aleutian Trench, STONELY (1967) described that the trench around the mainland was established since the late Cretaceous, and that the formation of the trench was accerelated in the Pliocene to Pleistocene period. SCHOLL (1975) said that the age of the wedge sediments of the North Pacific trenches are limited to the Middle and Late Pleistocene time, thus the age of trench formation is either young or it is very old as the wedge sediments have lost their wedge-shaped character. Von HUENE and SHOR (1969) suggested that it was not necessary to move the continental slope with trench, but crustal movement of the trench had to be closely connected with the movement of the slope or land parts, and it is a reasonable idea that the formation of the trenches was related with the upheaving of the continental shelf and Aleutian Peninsula since the Miocene time. The author consider that the crustal movement of continental slope and ocean floor took place at the same time since the Early Pliocene, and the trend of the movement of these parts was and uprising due to the expansion of the earth.

SCHOLL *et al.* (1968) described that to the south of Valparaiso the Peru-Chile Trench contains 500–700 m thickness of turbidites which abut on the basement, and the age of these sediments is not older than the age of the upheaving of the Andean Mountains in the Miocene to Pleistocene. STILLE (1955) also said that the age of formation of the Pacific trench is almost the same, the Late Pliocene. As the fossil trench of the eastern or western margins of the North Atlantic was formed at the Early Triassic period after the peneplanation stage of the Late Permian, the Pacific trenches were created in the Early Triassic period, grew up at the Cretaceous transgression stage (stage of ocean floor upheaving) and were completed with the epirogenic movement which produced the great sea-level uprising at the Early Pliocene and Early/Middle Pleistocene. BELOUSSOV and RUDITCH (1960) said that the fore-depression margin of the Japanese Islands had rapidly been depressed in the Pliocene period, and the region became a trench where the depressional movement was too rapid to be filled by the sediments. The relation between 'depression' after the Pliocene period and the formation of trench corresponds to the relation between the trench forming and ocean floor upheaving and the uprising of sea-level as the result of ocean floor uprising.

The data from geophysical surveys cannot conclude that the trench is a compressional field, and the trench is produced by subduction of the plate. Though TANNER (1973) urged that the trench is under a tensional force, without expansion of the earth it has to produce compressional field in other parts of the earth's surface. As WORZEL (1965) suggested both the trench and the ridge are tensional areas, then we should expect moderate expansion of the earth. WORZEL (1965) described extension of the earth's radius as 2–3%. It is an increase of radius of about 100–200 km. The author considers the expansion of the earth's radius is about 5 km since the Palaeozoic era resulting in an uprising of the sea-level. Such a magnitude of the earth's expansion cannot produce the continental drift.

Can the positive gravity anomaly and high terrestrial heat flow of the marginal swell be explained by the concept of plate subduction? Topographic high of the marginal swell also show the highest uprising of heat from the upper mantle. Though OLIVER (1970) said that the topography of "ridge and depression" on the oceanward slope of trench is produced by tensional force as a result of the buckling plate, this opinion cannot explain the origin of the positive anomaly and high heat flow. UYEDA (1975) explained the origin of positive gravity anomaly as a result of convergence of the lithosphere, but his opinion is not so presuasive.

5. Conclusion

The author urges that the trench was formed as a furrow left behind when the ocean floor upheaved. LUDWIG *et al.* (1966) described that the trench was produced where the thickness of earth's crust is thin and the thinness of the earth's crust was due to the faulting, warping with the crustal extension. From the view point of the crustal structure, the author considers that the trench is a place which is not so much affected by the expansional force because of the existence of the boundary between the continental and oceanic structures. WORZEL (1965) also said that the trench has a similar origin as that of a rift valley, i.e. tensional faulting. Though the author agrees with Worzel's opinion that the trench is a rift valley, the rift valley is not a valley caused by depression, rather it was produced as an abandoned valley when the ancient crust upheaved. KATZ (1975) maintained that the formational force of trenches —downwarping— can act only in a local area, and it relates to the development of the marginal part of the orogenic zone. The author agrees with the opinion that there is no need for plate tectonics to explain the formation of the trench, and the formation of the trench is related to the geological development of each regions. However he cannot agree with the opinion that formational force acts only in a limited area. The origin of trench is an upheaving of the ocean floor as a result of materials of the upper mantle rising. This also produced the domed elevation and rift valley in the shield regions, and produced the high mountains in the orogenic belt. The formational force of the trench is a global expansion of the earth.

Today, geologists describe the continental margin of the Pacific and Atlantic Oceans as active and passive margin respectively. The division may be done using the geological age of the margin as a basis for classification. This author divides the continental margin into two main classes, one is the Precambrian shield margin and the other is the Phanerozoic margin. The former has no trench and the latter has fossil or recent trenches. He believes it is a reasonable to divide the continental margin into active and passive, but he cannot agree with the opinion that the passive margin is a rift margin and the active margin is a subducting plate margin. Though the age of orogeny is not the same, every continental margin of an orogenic zone of the Phanerozoic eons has the same origin. Usually the trench was formed as a furrow left behind in the epirogenic stage, at the boundary between the continental and oceanic crusts.

Acknowledgements

The author appreciates assistance he has received, in preparing his manuscript, from Prof. A. SMITH, Bedford College and Prof. M. HAYASAKA, the Faculty of Marine Science and Technology, Tokai University.

References

BELOUSSOV, V. V. (1971): The crust and upper mantle of the ocean (transl. Assoc. Geol. Collab. Japan), Assoc. Geol. Collab. Japan, Tokyo, 326 p.

BELOUSSOV, V. V. and E, M. RUDICH (1960): Position of the island arc upon the development of the earth (transl. Y. KURODA), Green-Tuff Sosho, no. 2, 1-24.

BELYAEV, G. M. (1971): Fauna of deep-sea trenches and trends of its formation, in "The History of the World Ocean", 11-33, Isdatelistvo. Nauka, Moscow.

BENIOFF, H. (1949): Seismic evidence for the fault origin of oceanic deeps, Geol. Soc. Am. Bull., **60**, 1837-1856.

CHASE, R. L. and E. T. BUNCE (1969): Understanding of the eastern margin of the Antilles by the floor of the western North Atlantic Ocean, and origin of the Barbados Ridge, J. Geophys. Res., **74**, 1413-1420.

DE SITTER, L. L. (1956): Structural Geology, Mc-Grow Hill, N. Y., 552 p.

DUNBAR, C. O. and K. M. WAAGE (1969): Historical Geology (3rd ed.), John Wiley and Sons, N. Y., 556 p.

EMERY, K. O. (1960): The Sea off southern California, John Wiley and Sons, N. Y., 366 p.

EWING, J. I., N. T. EDGER and J. W. ANTOINE (1971): Structure of the Gulf of Mexico and Caribbean Sea, in "The Sea", 4(2), 332-358, Wiley Intersci., N. Y.

FISHER, R. L. (1975): Pacific type continental margin, in "The Geology of Continental Margins", 361-374, Springer-Verlag, N. Y.

FURUMOTO, A. S., G. P. WOOLLARD, J. F. CAMPBELL and D. M. HUSSONG (1968): Variation in the thickness of the crust in the Hawaiian Archipelago, in "The Crust and Upper Mantle of the Pacific Area", 94-111, Am. Geophys. Union Monogr.

GROW, J. A. (1973): Crustal and upper mantle structure of the central Aleutian arc, Geol. Soc. Am. Bull., **84**, 2169-2192.

HATHERTON (1975): Active continental margins and island arcs, in "The Geology of Continental Margins", 93-103, Springer-Verlag, N. Y.

HAYES, D. E. and M. EWING (1971): Pacific boundry structure, in "The Sea", **4**(2), 29-72, John Wiley and Sons, N. Y.

HERSEY, J. B. (1961): Findings made during the June 1961 cruise of Chain to the Puerto Rico Trench and Caryn Seamount, J. Geophys. Res., **67**, 1109-1116.

HIRAYAMA, J. and S. ASANO (1972): Central Asia and rivival mountains, Kagaku, **42**, 337-347.

HOSHINO, M. (1962a): The Pacific Ocean, Assoc. Geol. Collab. Japan, Tokyo, 136 p.

HOSHINO, M. (1962): Amino acids in sediment from the Japan Trench, J. Oceanogr. Soc. Japan, **18**, 1-3.

HOSHINO, M. (1964): Southwest Japan Trench, Marine Geol. (Tokyo), **1**, 10-15.

HOSHINO, M. (1969): On the relationship between the distribution of epicenter and the submarine topography and geology, J. Coll. Marine Sci. Tech., Tokai Univ., **3**, 1-10.

HOSHINO, M. (1970): Eustatic changes of sea level and the origin of trenches, in "Island Arcs and the Ocean", 155-177, Tokai Univ. Pr., Tokyo.

HOSHINO, M. (1975): Eustacy in relation to orogenic stage, 397 p., Tokai Univ. Pr., Tokyo.

HOSHINO, M. (1978): On unconformity, Preprint of Symposium on Unconformity, 1-43, Inst. Oceanogr., Tokai Univ., Shimizu.

HOSHINO, M. and K. HONMA (1966): Geology of submarine banks in the Japan Sea, Earth Sci., no. 82, 10-16.

IWABUCHI, Y. (1968): Topography of trenches east of the Japanese Islands, J. Geol. Soc. Japan, **74**, 37-46.

KANAMORI, H. (1972): Great earthquakes and island arcs, Kagaku, **42**, 203-211.

KATSUMATA, M. and C. R. SYKES (1969): Seismicity and tectonics of the western Pacific; Izu-Mariana-Caroline and Ryukyu-Taiwan regions, J. Geophys. Res., **74**, 5923-5948.

KATZ, H. R. (1975): Margins of Southwest Pacific, in "The Geology of Continents Margins", 549-565, Springer-Verlag, N. Y.

KUENEN, Ph. H. (1963): The negative isostatic anomalies in the East Indies (with experiments), Leidsche Geol. Mededeel., **8**, 196-214.

LANGSETH, M. Jr. and R. P. von HERZEN (1970): Heat flow through the floor of the world oceans, in "The Sea", 4(1), 299-352, Wiley-Intersci., N.Y.

LUDWIG, W. J., J. E. NAFE and C. L. DRAKE (1970): Seismic refraction, in "The Sea", **4**(1), 53-84, Wiley-Intersci., N. Y.

LUDWIG, W. J., J. I. EWING, M. EWING, S. MURAUCHI, N. DEN, S. ASANO, H. HOTTA, M. HAYAKAWA, T. ASANUMA, K. ICHIKAWA and J. NOGUCHI (1966): Sdements and structure of the Japan Trench, J. Geophys. Res., **71**, 2121-2137.

MAXWELL, J. C. (1975): Early western margin of the United States, in "The Geology of Continental Margins", 841-852, Springer-Verlag, N. Y.

MENARD, H. W. (1964): Marine Geology of the Pacific, McGraw-Hill, N. Y., 271 p.

MENZIES, J., J. IMBRIE and B. C. HEEZEN (1961): Further considerations regarding the antiquity of the abyssal fauna with evidence for a changing abyssal environment, Deep-Sea Res., **8**, 79-94.

MENZIES, R. J., R. Y. GEORGE and G. R. ROWE (1973): Abyssal Environment and Echology of the World Ocean, John Wiley and Sons, N. Y., 488 p.

MIZUNO, A., *et al.* (1975): Marine geology and geological history of Daito Ridges area, Kaiyo-Kagaku, **7**, 484-491.

MURAUCHI, S., N. DEN, S. ASANO, H. HOTTA, T. YOSHII, T. ASANUMA, K. HAGIWARA, K. ICHIKAWA, T. SATO, E. J. LUDWIG, J. I. EWING, N. T. EDGER and R. E. HOUTZ (1968): Crustal structure of the Philippine Sea, J. Geophys. Res., **73**, 3143-3171.

OLIVER, J. (1970): Structure and evolution of the mobile seismic belt, Phys. Planot. Interiors, **2**, 350-362.

OFFICER, C. B., J. I. EWING, R. S. EDWARD and H. R. JOHNSON (1957): Geophysical investigation in the eastern Caribean Venezuelan Basin, Antilles Island Arc and Puerto Rico Trench, Geol. Soc. Am. Bull., **68**, 359-378.

RENARD, V. and J. MASCLE (1975): Eastern Atlantic continental margins various structural and morphological types, in "The Geology of Continental Margins", 285-291, Springer-Verlag, N. Y.

SCHOLL, D. W. (1975): Sedimentary sequences in the North Pacific Trenches, in "The Geology of Continental Margin", 493-504, Springer-Verlag, N. Y.

SCHOLL, D. W., R. von HUENE and J. B. RIDLON (1968): Spreading of the ocean floor: undeformed sediments in the Peru-Chile Trench, Sci., 159, 869-871.

SEGAWA, J. and Y. TOMODA (1976): Gravity measurements near Japan and study of the upper mantle beneath the oceanic trench-marginal sea transition zones, in "The geophysics of the Pacific Ocean Basin and its Margin", 35-52, Am. Geophys. Union Monogr, **19**.

SHERIDAN, R. E. (1975): Atlantic continental margins, in "The Geology of Continental Margins", 323-342, Springer-Verlaag, N. Y.

SIESSER, W. G., R. A. SCRUTTON and E. S. W. SIMPSON (1975): Atlantic and Indian Ocean margins of South Africa, in "The Geology of Continental Margins", 641-654, Springer-Verlag, N. Y.

STILLE, H. (1955): Recent deformation of the earth's crust in the light of those of earlier epochs, in "Crust of the Earth", 171-191, Geol. Soc. Am., Spec. Paper **62**.

STONELY, R. (1967): The structural development of the Gulf of Alaska sedimentary province in southern Alaska, Geol. London Quat. J., **123**, 25-57.

SUESS, E. (1906): The Face of the Earth, **2**. 556 p, Oxford.

SYKES, L. S. and M. EWING (1965): The seismisity of the Caribbean region, J. Geophys. Res., **70**, 5065-5074.

TALWANI, M. and O. ELDHOLM (1973): Boundary between continental and oceanic crust at the margin of rifted continents, Nature, **241**, 325-330.

TANNER, W. F. (1973): Deep-sea trenches and the compression assumption, Bull. Am. Assoc. Petrol. Geol., **57**, 2195-2206.

The Res. Group for Daiichi Kashima Seamount (1976): Topography and geology of Daiichi Kashima Seamount off Inubo Cape, southeastern Honshu, Japan, Earth Sci., **30**, 222-240.

The Shipboard Scientist Party (1975): Site 298, Initial Rept., DSDP, **31**, 317-350.

The Shipboard Scientific Party (1976): Leg 43 of Glomar Challenger, Geotimes, December 1976, 18-21.

TSUCHI, R. and H. KAGAMI (1967): Discovery of Nerinid Gastropoda from Seamount Cblcoeb (Erimo) at the junction of Japan and Kurile-Kamchatka Trenches, Rec. Oceanogr. Works in Japa, **9**, 1-6.

UDINTSEV, G. B. (1967): Geomorphology of the floor of the Pacific Ocean, in "Intl. Dict. Geophys.", **1**, 656-667.

UMGROVE, J. H. F. (1947): The Pulse of the Earth, 358 p., Martinus Niihoff, Hague.

UYEDA, S. (1975): Northwest Pacific trench margins, in "The Geology of Continental Margins", 473-491, Springer-Verlag, N. Y.

VAN BEMMELEN, R. W. (1954): Mountain Building, Martinus Niihoff, Hague, 177 p.

VENING MEINESZ, F. A. (1930): Maritime gravity survey in the Netherlands East Indies, tentative interpetation of the results, Koninkl. Ned. Akad. Wetenshp., Proc., **33**, 566-577.

VENING MEINESZ, F. A. (1948): Gravity expedition at sea, 1923-1938, Publ. Neth. Geol., Delft, **4**.

Von HUENE, R. (1975): Modern trench sediments, in "The Geology of Continental Margins", 207-211, Springer-Verlag, N. Y.

Von HUENE, R. and G. G. SHOR, Jr. (1969): The structure and tectonic history of the eastern Aleutian Trench, Geol. Soc. Am. Bull., **80**, 1889-1902.

WATANABE, T., B. EPP, S. UYEDA, M. LANGSETH, and M. YASUI (1970): Heat flow in the Philippine Sea, Tectonophys., **10**, 205-224.

WATTS, A. B., M. TALWANI and J. R. COCHRAN (1976): Gravity field of the Northwest Pacific Ocean Basin and its margin, in "The Geophysics of the Pacific Ocean Basin and its Margin", 17-34, Am. Geophys. Union Monogr, **19**.

WORZEL, J. L. (1965): Deep structure of coastal margins and mid-oceanic ridges, in "Submarine Geology and Geophysics", 335-361, Butterworths, London.

WORZEL, J. L. (1975): Standard oceanic and continental structure, in "The Geology of Continental Margins", 59-66, Springer-Verlag, N. Y.

YASUI, M., D. EPP, K. NAGASAKI and T. KISHII (1970): Terrestrial heat flow in the seas around the Nansei Shoto, Tectonophysics, **10**, 225-234.

ZENKEVICH, L. A. and J. A. BRISTEIN (1960): On the problem of the antiquity of the deep-sea fauna, Deep-Sea Res., **7**, 10-23.

海　溝　の　成　因

星　野　通　平

要旨： 海溝の地形・地質・地球物理学的諸特徴は，海溝が圧縮の場において形成されたものではなく，むしろ，張力の場において形成されたものであることを示している。筆者は，海溝は地球の膨脹からとり残された凹地である，と主張する。つまり，地殻の弱線にそって膨脹（隆起）力が作用せず，膨脹（隆起）する大陸・大洋地殻のあいだにとり残された凹地が海溝である。現世および化石海溝は，顕生代の造山帯にそって分布しており，このことは顕生代が塩基性（海洋性）火成岩の活動時代であることに照応しており，太平洋に現世海溝が多数分布することは，太平洋の海洋性地殻の活動（隆起）が一ばん新期のものであることを物語っている。

La mer (Bulletin de la Société franco-japonaise d'océanographie)
Tome 16, N° 3, pp. 124 à 136, Août 1978

Biological and Ecological Studies on the Propagation of the Ormer, *Haliotis tuberculata* LINNAEUS

I. Larval Development and Growth of Juveniles*

Yasuyuki KOIKE**

Résumé: L'élevage du naissain d'ormeau, *Haliotis tuberculata* fut réalisé durant la campagne 1973 et 1974 au Centre Océanologique de Bretagne (CNEXO-COB) à Brest, France.

La ponte a été obtenue par stimulation thermique en eau de mer courante. Un grand nombre d'oeufs fécondés a pu être obtenu au début août 1973.

Le développement larvaire et la croissance de naissain ont été suivis pendant 435 jours après la fécondation. Les stades importants du développement sont illustrés au moyen de figures.

La taille moyenne de 2840 individus au 435^e jour était 2,12 cm de longueur et 1,28 cm de largeur.

1. Introduction

The ormer (ormeau or oreille de mer in French), *Haliotis tuberculata* LINNAEUS, is a European abalone, and is found along the north-west coasts of France, from the south coasts of the Brittany Peninsula to the west coasts of the Normandy Peninsula, as well as around the British Channel Islands (Fig. 1.). It grows to a maximum size of about 12 cm in shell length and has always been highly esteemed. There has been a special ormer fishery industry since ancient times. Above all, in Guernsey in the Channel Islands, the ormer fishery was commercially important (53 tons of total catch in 1967), and from here the ormer used to be exported to France (GIRARD, 1972). The ormer shellfishery there has long been operated under strict regulations, but nevertheless the natural stocks have decreased remarkably in recent years so that a ban had to be placed on all ormer fishing. Even in France measures have been taken to protect ormer stocks and fishing by divers has been prohibited since 1965. At the present time the only ormer fishery permitted is shoregathering at the period of the spring

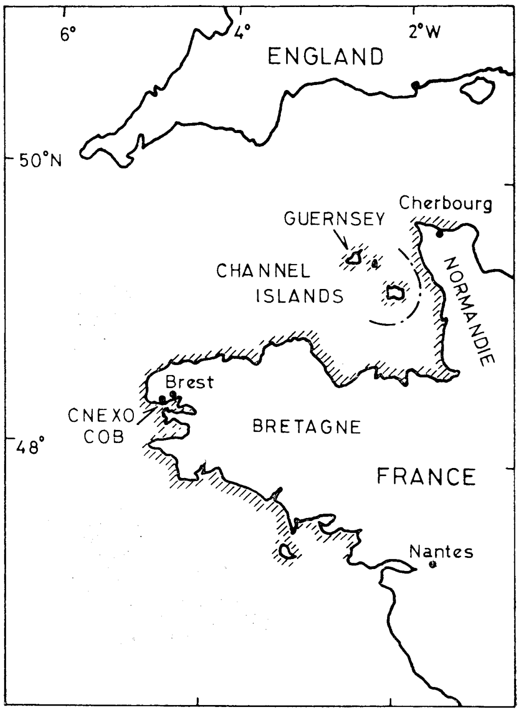

Fig. 1. Range (hatched area) of the European abalone, *Haliotis tuberculata*.

* Received May 29, 1978

** Centre Océanologique de Bretagne (Aquaculture), CNEXO, Brest, France.
Present address: Laboratory of Animal Ecology, Tokyo University of Fisheries, Konan 4-5-7, Minato-ku, Tokyo, 108 Japan.

tides.

The study of the basic biology of this shellfish has a long history; BOUTAN (1899) describes its early development in relation to asymmetry. STEPHENSON (1924) makes an investigation to seek the reasons why ormer stocks decreased around Guernsey. CROFTS (1929, 1937) examines its basic biology and larval development with regard to torsion. FORSTER (1962, 1967) carries out ecological studies by diving and tagging experiments to make clear its distribution, movement and growth around the coasts of Guernsey. GIRARD (1972) makes a histological study of gonad development as well as other aspects of ormer reproduction. However, no work had ever been done concerning the artificial propagation of this species.

The present author began trials in June 1973 for the artificial induction of spawning of the species in question at the Centre Océanologique de Bretagne, CNEXO (CNEXO-COB) in Brest. The aim was to develop a technique for getting a good number of seedlings for mass production or tank rearing on a large scale. This study reveals some interesting facts new to science, and above all it makes clear all the aspects of early development and growth of the ormer for 435 days after fertilization through spat and juvenile stages under artificial conditions.

2. Material and methods

The adult ormers for the rearing experiments were taken by diving in Brest Bay during the period from the end of June to the beginning of August in 1973.

The procedure employed in the experiment is summarized as follows:

Spawning was induced in the laboratory by means of exposure to air, or of fluctuating water temperature acting as a stimulant on the mature adults. The aquarium used for spawning for both sexes was made of polyethylene, rectangular in shape, and $60 \times 40 \times 25$ cm in size. After emission of a quantity of sperm, male shells were removed from this tank and placed in other tanks.

The eggs were fertilized in the tank by the sperm already emitted therein. When necessary, some extra sperm was added from the other tanks.

After being washed several times, fertilized eggs were reared in another tank of the same size and type. At the trochophore stage, ormer larvae were removed to a series of larger tanks, $200 \times 50 \times 25$ cm in size. During the first 12 days, the larvae were kept in still water which was not changed at all. Furthermore, during this time very little aeration was applied.

After the 13th day and for the rest of the experiment, larvae were kept in running water; water temperature was in the range of $20° \pm 1°C$, and specific gravity between 1.0252 and 1.0267.

At the time of settlement of the larvae, collectors were set in the tanks. They were made of transparent plastic plate, on which diatoms had grown to form a thin film or layer. The water was enriched by adding to it "Conway solution" ($1\ cc/l$) and Sodium metasilicate, $Na_2SiO_3 \cdot 5H_2O$, ($30\ mg/l$) to promote the growth of diatoms. An additional feeding of *Tetraselmis suecica* was found to be very effective.

After the young abalones started to grow up and to move from the collectors, a number of pieces of rock and U shaped plastic plates were placed in the tanks as shelters for them. The plastic plates were $30 \times 20 \times 2$ cm in size. Young abalones were then fed first on *Ulva lactuca* in small pieces and later on a mixture of *Laminaria digitata*, *Saccorhiza polychides* and *Rhodymenia palmata*.

3. Results and considerations

Induction of spawning

For the trials for inducing spawning, about 30 adult ormers were collected on June 29th, 1973. All spawned during the night of 29th–30th June and could not be used for the experiments. In this case water temperature in the tanks was maintained at the natural water temperature of 17.2°C. However it took 40 minutes to transport the ormers from the collecting site to the laboratory, and stimulation caused by drying during this time will have had some effect on inducing spawning. From this result it became clear that mature adults are easily stimulated and that collected ormers should be induced to spawn on the same day they are collected. Following this method,

Table 1. Conditions for induction of spawning carried out on 1st August, 1973.

Activity \ Items	Time	Temperature (°C)
Collection of adults	12 hr 10 min	17.5 (open sea)
Stimulation in air	during 40 minutes	28.7 (air)
Beginning of induction process in heated water	13 hr 30 min	25.0 (water)
Emission of sperm (3♂)	15 hr 45 min	21.0 (water)
Spawning (2♀)	15 hr 55 min	21.0 (water)
Fertilization	16 hr 00 min	21.0 (water)
Number of eggs obtained	1,120,000	——

normal experiments were carried out on 1st August.

The ormers used for the experiment were 21 females and 11 males ranging in shell length from 7.8–9.5 cm. The procedure followed for inducing spawning is shown in Table 1. Mature adults were collected at 12 h 10 p.m. It took 40 minutes to transport them to the laboratory, that is 40 minutes stimulation by drying. The air temperature at this time was 28.7°C and the water temperature in the tanks was maintained at 26.0°C so as not to have too great a temperature difference. Stimulation by fluctuations of water temperature was started at 13 h 30. Water temperature was gradually decreased by adding running water of 21.0°C. After 2 hrs 15 min, when the water temperature had decreased to 21.0°C, three males started to spawn and after 2 hrs 25 min, two females spawned at the same water temperature (Fig. 2). The number of eggs was 590,000 (shell length 7.8 cm) and 646,000 (shell length 8.2 cm). Of the total of 1,236,000 eggs, around 1,120,000 were viable and could be used for rearing experiments.

Concerning attempts to obtain fertilized eggs of *H. tuberculata*, STEPHENSON (1924) succeeded at Guernsey on 1st August, using mature adults collected the day before and CROFTS (1937) at Roscoff, France, succeeded in getting fertilized eggs from natural spawning in the laboratory on 22nd July. From these results and that of the present study it is clear that induction of spawning with this species is easier than with Japanese abalone *H. discus discus* and *H. sieboldii* (INO, 1952), *H. diversicolor supertexta* (OBA, 1964) and *H. discus hannai* (KIKUCHI, 1964).

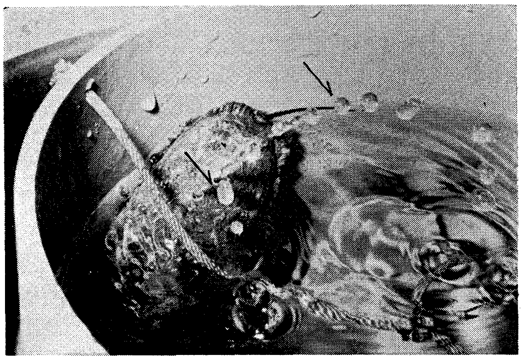

Fig. 2. Spawning of *Haliotis tuberculata* in a tank. A row of water drops (arrows) can be seen here ejected by the mother shell through its respiratory pores; ovae are carried in these drops.

Early development

The fertilized eggs are spherical and have a diameter of 0.21 mm including egg membrane. The yolk has a diameter of 0.17 mm. With a water temperature of 20°C±1°C, the first polar body appeared after a few minutes. Very soon after, the second polar body appeared, but as with *H. discus discus* (INO, 1952), in many cases no second polar body was observed (Plate I–1). The time sequence for egg development following fertilization was as follows:

After 1 hr 10 min–1 hr 50 min, the first division took place along the vertical axis of the egg (Plate I–2). After 1 hr 40 min–2 hrs 10 min, the second division took place along the same axis (Plate I–3, 4). After 2 hrs 20 min, the third division took place just above horizontal axis of the egg and at that time the differentiation between micromeres and macromeres could be made and the micromeres were seen to move around the macromeres in a clockwise direction

(Plate I-5). After 3 hrs 15 min, the fourth division took place and the direction of torsion was observed to be counterclockwise (Plate I-6). After 5 hrs, the embryo reached the morula stage (Plate I-7), and after 8 hrs 30 min-9 hrs, reached the gastrula stage after passing through the blastula stage. After 10 hrs, at the trochophore stage, the cilia appeared and intermittent rotating movement was observed in the egg membrane. After 13 hrs, hatching took place and the size of newly hatched larvae was 0.2× 0.155 mm and some larvae were observed to have already secreted their transparent larval shell from the shell gland (Plate I-8). There are various opinions in the literature concerning the apical tuft in this species. According to BOUTAN (1899) no apical cilia were observed at any stage of development. CROFTS (1937) reports that the trochophore has no apical cilia but the veliger has a transitory apical tuft. In the present experiment it was observed that from trochophore stage just before hatching until veliger stage just before the velum divides, this species has an apical tuft (Plates I-8, 9 and II-1, 2).

The trochophore moved slowly on the bottom of the tank for the first two hours. Then they began to float up to the surface and they were observed to be swimming up and down between the middle and surface layers grouped in several vertical columns. At this time they showed positive phototactice and it was easy to transfer them to another tank by using a light to attract them to one corner for siphoning. Concerning phototactice in *Haliotis* species, OBA (1964) reports little evidence of positive phototactice in *H. diversicolor supertexta*, INO (1952) observed strong positive phototactice in *H. discus discus* but only moderately strong for *H. sieboldii*. It appears that this behaviour varies according to species.

After 18-20 hrs, the larval shell had developed and the larvae reached veliger stage. With the growth of the larval shell the cells of the visceral hump developed and the velum was formed (Plate I-9). After 35-38 hrs, veliger torsion was complete, and the foot and the operculum developed. At that stage the larvae were already able to retract themselves into the shell indicating the development of the muscle (Plates I-10 and II-1, 2). In the literature, the stage at which retraction first was observed differs according to species. In the case of *H. discus discus* (INO, 1952) and *H. diversicolor supertexta* (OBA, 1964) retraction first was observed in veligers only after division of the velum and appearance of the eyes and rudiments of tentacles. This indicates that retraction starts later for these two species than in the case of *H. tuberculata*. The veligers of *H. tuberculata* were observed to swim actively but to react immediately by retracting

Table 2. Comparison of development characteristics among *Haliotis tuberculata* (H. t.), *H. discus* (H. d.), *H. sieboldii* (H. s.), *H. gigantea* (H. g.) and *H. diversicolor supertexta* (H. d. s.).

Items	H. t. present study	H. d. INO (1952)	H. s. INO (1952)	H. g. MURAYAMA (1935)	H. d. s. OBA (1964)
Diameter (mm) of fertilized egg	0.21	0.23	0.28	0.27	0.20
Length (mm) of larval shell	0.26	0.29	0.29	0.36	0.254
Trochophore stage (hours after fertilization)	10	14	15	14	4.67
Time (hours) required for hatching, (in given water temperature, °C)	13 (20)	20 (16-17)	18 (16-18)	21-22 (16-18)	6 (26.2)
Torsion (hours)	35-38	45-46	35	40-43	13
Appearance (days) of eyes and cephalic tentacles	2	2.5	2.5	10	0.7-0.8
Appearance (days) of epipodes	3.5	5	4	28	1.6
Time (days) required before creeping	3.5-5	6-10	4-7	7-10	1.8-1.9
Appearance (days) of peristomal shell	5-6	10-11	10	10	2.7
Appearance (days) of first respiratory pore, (shell length, mm)	38-40 (2.0-2.3)	130 (2.3-2.5)	—	—	23 (1.8-1.9)

into their shell when subjected to any external stimulation. At this stage the shell had an irregular moiré pattern which differed considerably from the patterns on the shells of veligers of *H. discus discus* (INO, 1952) and *H. diversicolor supertexta* (OBA, 1964), (Plate I-10).

After two days and a half, the velum separated into two parts and rudiments of cephalic tentacles and eyes appeared at the center of each part (Plate II-3, 4). At this stage the larval shell was complete and measured 0.26 mm in length which is a little larger than *H. diversicolor supertexta* and smaller than *H. gigantea*, *H. sieboldii* and *H. discus discus* (Table 2). The veligers were observed to swim in rotating fashion near the bottom of the tank resting on the bottom of the tank from time to time and twisting their foot. When they retracted into their shell, the foot was folded at its centre. The edge of the mantle also developed and could be recognised through the transparent larval shell as an arch shaped fold. Gradual development of the cephalic tentacles with papillae was then observed and the rudiments of epipodial tentacles appeared on both sides of the foot.

By the end of the third day, cilia started to develop on the pedal sole and the first signs of settlement behaviour were observed. Many of the larvae could change the shape of their foot and attach it to an available surface but they were unable to start creeping. After 4-5 days most of the larvae were seen to be creeping around. At this time the papillae of the cephalic tentacles had become more numerous and sensory threads and a pale green pigmentation were observed. The velum had diminished in size and the snout had begun to protrude at the front of the velum. The statocyst was observed between the head and foot with five or six grains all grouped together at the centre forming the statolith (Plate II-5, 6).

On the sixth day the cilia on the velum disappeared and the secretion of the peristomal shell began on the right side of the aperture of the larval shell. At this time the snout was well formed and the pedal sole had become more developed allowing the larvae to creep around actively. The movement of the heart was also apparent (Plate III-1).

On the ninth day the spat measured 0.37 mm in shell length including 0.18 mm of the newly secreted peristomal shell on which wave-like lines were conspicuous. At this time the number of papillae on the cephalic tentacles increased. Movement of the radular was observed for the first time and the first ciliary lobe appeared behind the right eye-stalk (Plate III-2). The exact timing of the loss of the operculum was never fully established but it was still present at this stage.

On the sixteenth day the spat measured 0.47 mm in shell length and the shape became flat with the gradual growth of the peristomal shell covering the right side of the body. The thickness of the shell had also increased. On the surface of plastic collectors, the spats were recognizable, when observed with the naked eye, as white dots with a pale brown patch over the visceral hump. The length of the cephalic tentacles increased and the number of papillae on them had increased also. The first development of the left ctenidium was recognized in the branchial chamber (Plate III-3). After that the first ciliary lobe became gradually larger and then the second ciliary lobe appeared behind the first one. The movement of their cilia was observed to produce a water current flowing from the left side of the head to the right side (Plate III-4). These ciliary lobes continued their function for the following two weeks (Plate V-2), but at the time that the cleft of the first respiratory pore started to form in the shell (about the 30th day) their size began to diminish (Plate V-4), and by the 40th day, when the first respiratory pore was completely formed, only traces of them were left and their function ended. From this fact, it can be considered that, as suggested by CROFTS (1937), INO (1952) and OBA (1964), these ciliary lobes act as respiratory organs having the function of circulating and discharging the water in the branchial chamber.

On the 25th day the spat measured 0.98 mm in shell length and 0.89 mm in shell breadth and the shell shape had become almost circular. On the surface of the shell, brown patterns appeared in patches. The cephalic tentacles had become longer and the number of their papillae became more numerous. The epipodial tentacles had developed in four pairs and the dark line of the intestine could be seen through the shell (Plate IV-1, 2). The left ctenidium in the branchial chamber had developed and the number of branches on it had increased (Plate V-1). On the opposite side of the head, two ciliary lobes still moving actively could be recognized (Plate V-2). At this time feeding behaviour was very active and the areas of grazing on the diatom film could be seen as white patches on the surface of the collectors (Plate V-3).

From about the 30th day, a cleft in the margin of the shell on the right side of the head was observed and, by 38th-40th day, the cleft had become a hole in the shell and the first respiratory pore was formed (Plate IV-3, 4). At this time the spat measured 2.0-2.2 mm in shell length and there were reddish brown patches on the surface of the shell and 3 or 4 ridges running from the front end to the apex of the shell were seen. The visceral hump could be seen like a violet patch through the shell. The eye stalks had grown longer than the two ciliary lobes which had nearly disappeared and the left ctenidium had increased the number of its branches (Plate V-5). At the aperture of the snout the radial folds had formed running from the center to the margin of the aperture and the active movement of the radular was observed (Plate V-6). The number of the epipodial tentacles of *H. tuberculata* at the time of the formation of the first respiratory pore was 14 or 15 pairs; this was more than *H. discus discus* which had 8 or 9 pairs (INO, 1952) and about the same number as *H. diversicolor supertexta* (OBA, 1964).

Concerning the stage at which the formation of the first respiratory pore takes place, observations for several species, as described in the literature to which reference has already been made, are shown in Table 2. For *H. tuberculata* it is earlier than *H. discus discus* but later than *H. diversicolor supertexta*. The present observations for *H. tuberculata* coincide with those of CROFTS (1937) who described that it takes place two months after fertilization at a size of 2 mm in shell length. In the case of *H. discus hannai* (KIKUCHI, 1964) it takes place on the 42nd day when the shell measures 2.5 mm in shell length, which is a little later than *H. tuberculata*.

After about 50 days, the spat reached a size of 2.5-2.6 mm in shell length and the epipodial tentacles numbered 20-22 pairs. At this time the shell had two respiratory pores and on the inside of the shell the pearly lustre was first observed.

By the 85th-90th day, the spat had reached a size of 3.1-3.3 mm in shell length and there were 26-27 pairs of epipodial tentacles. Four respiratory pores were formed but the first one was already closed. The flame-like patterns on the surface of the shell had changed in colour from reddish brown to violet. The visceral hump also changed colour to deep violet which was seen through the shell. At this time many spats were observed to be feeding on the green seaweed, *Ulva* spp., growing on the collectors.

At about 160th day, they reached a size of 6.2 mm in shell length and the number of respiratory pores had increased to 9-10 of which 4 or 5 pores were open. The cephalic tentacles had grown to about the same length as the shell and the epipodial tentacles had become more numerous (Plate VI-1). The number of respiratory pores continued to increase with shell growth, but closed gradually except for the 3-6 pores nearest the front margin of the

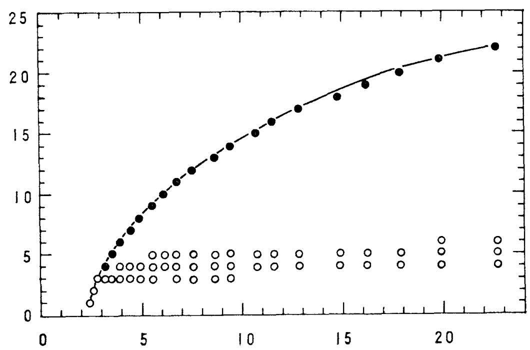

Fig. 3. Relationship between number of respiratory pores (ordinate) and shell length (abscissa, mm) in young *Haliotis tuberculata*. ●; Total number of pores, both open and closed, ○; Number of open pores.

shell which were functioning. The relation between growth and the number of respiratory pores is shown in Fig. 3.

Concerning changes in colour of the *Haliotis* shell, INO (1952), SAKAI (1962) and OBA (1964) describe that the colour of the shell of *H. discus discus*, *H. discus hannai* and *H. diversicolor supertexta* changed with the different seaweed on which they fed. This phenomenon was also clearly seen in *H. tuberculata*. The colour of the shell was reddish brown when they were feeding on diatoms, but the colour changed to green when feeding on *Ulva* spp. and *Laminaria* spp., and changed to red when feeding on *Rhodymenia* spp. (Plate VI-2). This may be useful as a way of distinguishing between groups of juveniles each having different patterns on their shells when they are released on the sea bed.

The growth of juveniles is shown in Fig. 4. By the 435th day after fertilization they reached an average size of 21.153 ± 3.872 mm in shell length and 12.766 ± 2.246 mm in shell breadth. The number of living juveniles at that time was 2,840.

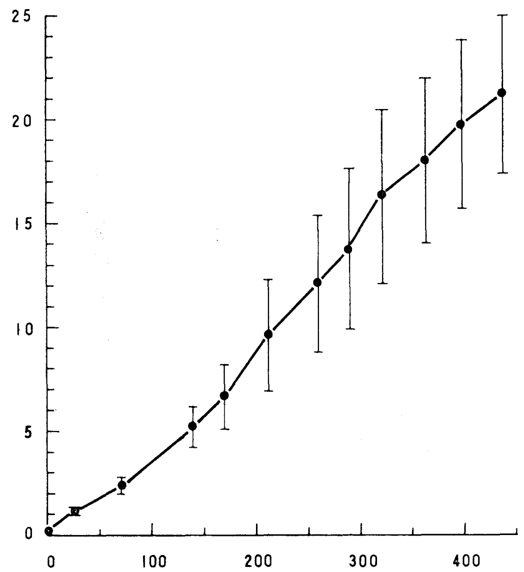

Fig. 4. Growth in shell length (ordinate, mm) of young *Haliotis tuberculata* during 435 days (abscissa) after fertilization (0 days). Range of shell length is represented by a vertical line.

4. Summary

Tank rearing of the European abalone, *Haliotis tuberculata* was carried out from 1973 to 1974 at Laboratory of Centre Océanologique de Bretagne (CNEXO-COB) in Brest, France.

Spawning was promoted by stimulation using fluctuations of water temperature and fertilized eggs were obtained in August 1973. Their development was observed for 435 days after fertilization. The results are summarized as follows:

1) Mature adults of *H. tuberculata* have a tendency to spawn more easily following stimulation than three species of Japanese abalones, *H. discus discus*, *H. discus hannai* and *H. diversicolor supertexta*.

2) The eggs are spherical and each is enclosed within a thick gelatinous coating. Their size is 0.21 mm in diameter including egg membrane, and yolk is 0.17 mm in fertilized condition.

3) The division of the egg is total, unequal and spiral.

4) At a temperature of 20°C, the trochophore escapes from the egg membrane within 13 hours after fertilization. Size is about 0.2 mm in length. The hatched larvae are positively phototactic and swim near the surface of the water.

5) The apical tuft is visible at all stages from trochophore before hatching to veliger before the velum separates into two parts.

6) The change from trochophore to veliger stage takes place within 20 hrs. and torsion takes place 35–38 hrs. after fertilization.

7) The rudiment of cephalic tentacles, eyes, foot and operculum appear in the post-tosional veliger. The larval shell is 0.26 mm long.

8) The transition from pelagic to benthic life takes place within a period varying from 3.5 to 5 days after fertilization. The velum is then absorbed and the peristomal shell is secreted along the outer lip of the aperture of the larval shell.

9) The first ciliary lobe appears 9 days after fertilization and the second one appears 7 days later.

10) The first respiratory pore appears 38–40 days after fertilization when the larvae are 2.0–

2.3 mm in shell length. At this time the function of the two ciliary lobes is lost.

11) The juveniles change the colour of their shell when they are fed on different sorts of seaweeds, e.g. diatomes: reddish brown, *Ulva* and *Laminaria*: green, *Rhodymenia*: red.

12) The juveniles reached a size of 2.12 cm in shell length and 1.28 cm in shell breadth on the 435th day.

Acknowledgement

The author wishes to acknowledge the continuing guidance and encouragement of Prof. T. IWAI of Kyoto University during his study. He is also greatly indebted to Prof. Y. UNO of Tokyo University of Fisheries for suggesting this subject of research and for stimulating interest in it. Sincere thanks are due to many former colleagues, especially Dr. J. P. FLASSCH, at the Centre Océanologique de Bretagne, Brest; without their assistance this study could not have been completed. The author would also like to express his special appreciation to Messrs. Y. NORMANT and C. AVELINE at the Centre for all the help they gave him. Finally he would like to thank Prof. K. TAKAGI and Mr. J. J. WALFORD, visiting researcher, of Tokyo University of Fisheries, for their kind suggestions with respect to the format of this text.

References

BOUTAN, L. (1899): La cause principale de l'asymetrie des Mollusques Gastéropode. Arch. Zool. Exp., (3) VII, 270-331.

CROFTS, D. R. (1929): *Haliotis.* L. M. B. C. Mem. typ. Br. Mar. Pl. Anim. **29**, 1-174.

CROFTS, D. R. (1937): The development of *Haliotis tuberculata*, with special reference to organogenesis during torsion. Phil. Trans. R. Soc. Lond. Ser. B, **228**, 219-268.

FORSTER, G. R. (1962): Observation on the ormer population of Guernsey. J. Mar. Biol. Ass. U. K., **42**, 493-498.

FORSTER, G. R. (1967): The growth of *Haliotis tuberculata:* Results of tagging experiments in Guernsey, 1963-65. J. Mar. Biol. Ass. U. K., **47**, 287-300.

GIRARD, A. (1972): La reproduction de l'ormeau *Haliotis tuberculata L.* Rev. Trav. Inst. Pêches Marit., **36**(2), 163-184.

INO, T. (1952): Biological studies on the propagation of Japanese abalone (Genus *Haliotis*). Bull. Tokai Reg. Fish. Res. Lab., **5**, 1-102. (In Japanese with English summary).

KIKUCHI, S. (1964): Study on the culture of abalone, *Haliotis discus hannai* INO. Cont. 1964 Peking Symp. Gen 041, 185-202.

MURAYAMA, S. (1935): On the development of the Japanese abalone, *Haliotis gigantea.* J. Coll. Agric. Tokyo, **13**(3), 227-233.

OBA, T. (1964): Studies on the propagation of an abalone, *Haliotis diversicolor supertexta* LISCHKE-II. On the development. Bull. Jap. Soc. Sci. Fis., **30**(10), 809-819. (In Japanese with English summary).

SAKAI, S. (1962): Ecological studies on the abalone, *Haliotis discus hannai* INO-I. Experimental studies on the food habit. Bull. Jap. Soc. Sci. Fish., **28**(8), 766-779. (In Japanese with Englsih summary).

STEPHENSON, T. A. (1924): Notes on *Haliotis tuberculata.* J. Mar. Biol. Ass. U. K., **13**(2), 480-495.

欧州産アワビ, *Haliotis tuberculata* LINNAEUS の増殖に関する生物学的および生態学的研究

I. 初期発生および稚貝の成長

小 池 康 之

要旨: 人工採苗によって得られたヨーロッパ産アワビ *Haliotis tuberculata* の稚貝を435日間飼育し，その初期発生および成長過程を明らかにし詳細に図示した (Pls. I-VI)。

本種は日本産アワビ属と比較して，産卵誘発刺激に反応しやすい傾向を示す。卵は水温 20°C において受精後約13時間で担輪子に成長し孵化する。担輪子は顕著な走光性を示す。受精後約 20 時間で被面子に達し，35～38 時間後に捩れ (torsion) が起る。頂毛は孵化直前の担輪子から面盤 (velum) が二葉に分化する直前の被面子に至る各期に認められる。受精後 50～60 時間の被面子には頭部触角の起源，眼および蓋が形成され，その時期の幼殻の大きさは 0.26 mm である。

被面子は受精後 3.5～5 日で底生期に達し，この時期に上足突起の起源が現われる。6 日目には面盤が退化して周口殻の分泌が始まる。第一繊毛葉は 9 日目に，第二繊毛葉は 16 日目までに形成される。最初の呼水孔は 38～40 日後，殻長 2.0～2.3 mm で形成され，この時期に繊毛葉が退化してその機能を失なう。

餌料海藻の変化に伴い，貝殻の色彩に明瞭な変化が認められる。

飼育稚貝は 435 日後に殻長 2.12 cm，殻幅 1.28 cm に成長する。

EXPLANATION OF PLATES I-VI

PLATE I

1. Fertilized egg with polar bodies. 0.21 mm in diameter including egg membrane; yolk, 0.17 mm in diameter.
2. Egg in 2 cell stage, 1 hr 10 min–1 hr 50 min after fertilization.
3. Egg at the beginning of second cleavage, 1 hr 40 min.
4. Egg in 4 cell stage, 1 hr 50 min.
5. Egg in 8 cell stage (animal pole view), 2 hrs 20 min.
6. Egg in 16 cell stage (animal pole view), 3 hrs 50 min.
7. Embryo in morula stage, 4 hrs 50 min.
8. Embryo in trochophore stage, 13 hrs. 0.15×0.20 mm.
9. Larva in early veliger stage, 20 hrs 20 min. 0.20 mm in diameter.
10. Larva in veliger stage after torsion, 38 hrs 30 min–40 hrs.

PLATE II

1. Larva in veliger stage after torsion, 38 hrs 30 min–40 hrs.
2. Same specimen as seen in Plate II–1 (ventral view).
3. Veliger larva in late swimming stage, 2.5 days. 0.26 mm in diameter of shell.
4. Same specimen as seen in Plate II–3; body retracting into shell.
5. Veliger larva in early benthic stage, 4.5 days. 0.26 mm in diameter of shell.
6. Same specimen as seen in Plate II–5 (ventrolateral view).

PLATE III

1. Creeping larva, beginning to secrete peristomal shell (ventral view), 6 days. 0.27 mm in diameter.
2. Creeping larva (dorsal view), 9 days. 0.37 mm in shell length.
3. Creeping larva, beginning to develop epipodes (ventral view), 16 days. 0.47 mm in shell length.
4. Same specimen as seen in Plate III–3, showing ciliary lobes (ventral view).

PLATE IV

1. Creeping larva having much more developed epipodes (dorsal view), 25 days. 0.98 mm in shell length.
2. Same specimen as seen in Plate IV–1 (ventral view).
3. Young abalone having first respiratory pore (dorsal view), 40 days. 2.2 mm in shell length.
4. Same specimen as seen in Plate IV–3 (ventral view).

PLATE V

1. Developing ctenidium (ventral view), 25 days.
2. Two ciliary lobes and radular in movement (ventral view), 25 days.
3. Larvae (white dots) on the collector, 25 days.
4. Two ciliary lobes having lost their functions (ventral view), 30 days.
5. More developed ctenidium (ventral view), 25 days.
6. Snout and radular in movement (ventral view), 35 days.

PLATE VI

1. Young abalone (dorsal view), 160 days. 6.2 mm in shell length.
2. Young abalone with different colour bands (dorsal view), 13 months. 20.3 mm in shell length.

LEGEND OF ABBREVIATIONS

ap. t.	apical tuft	l. sh.	larval shell
ceph. t.	cephalic tentacle	m.	muscle
c. l. 1	first ciliary lobe	mant.	mantle
c. l. 2	second ciliary lobe	op.	operculum
ct.	ctenidium	p. b.	polar body
e. c.	endodermal cell	ped. gl. p.	posterior pedal gland
e. m.	egg membrane	ped, so.	pedal sole
ep.	epipode	pr. g.	prototrochal girdle
ep. t.	epipodial tentacle	pst.	peristomal shell
f.	foot	rad. s.	radular sheath
h.	heart	resp. p.	respiratory pore
int.	intestine	s.	snout
l.	liver	stat.	statocyst

PLATE I

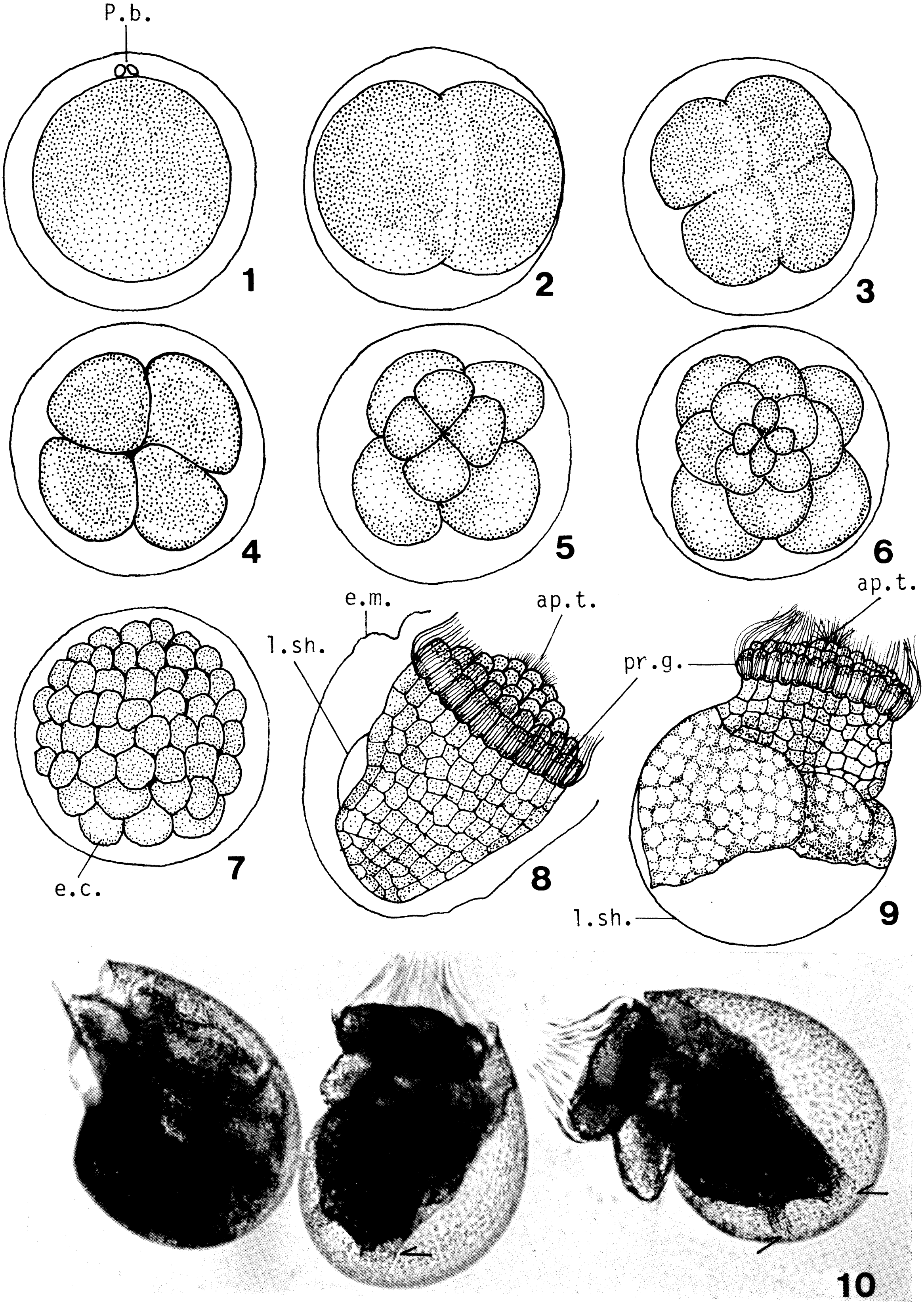

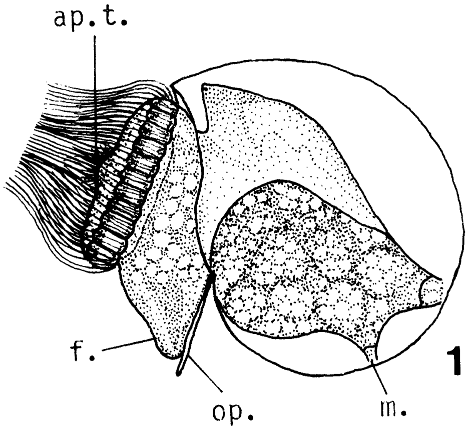

1

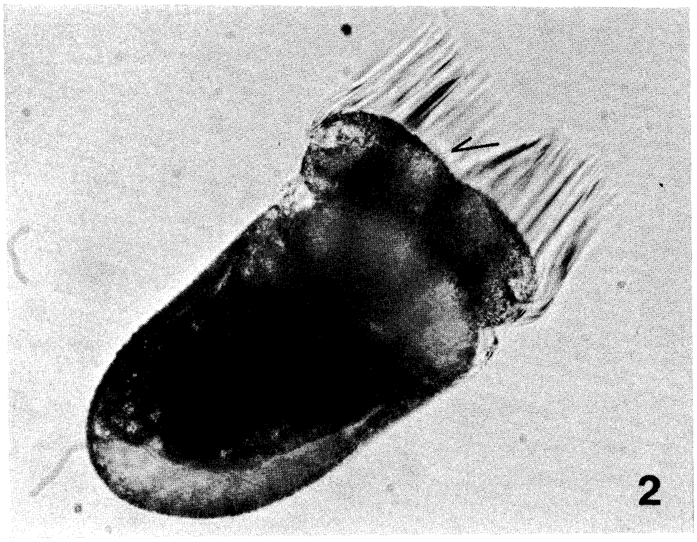

2

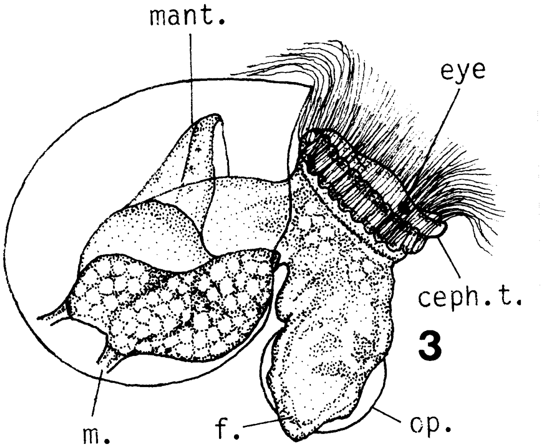

3

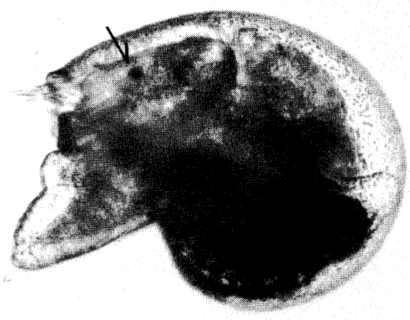

4

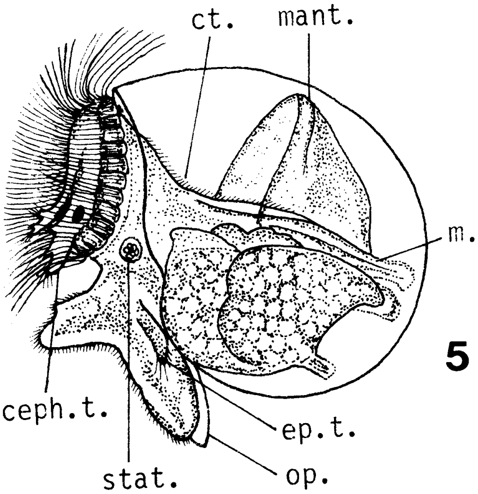

5

6

PLATE III

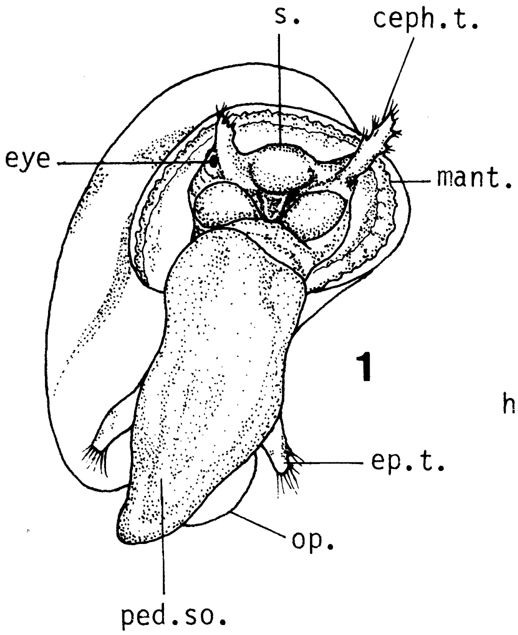

1

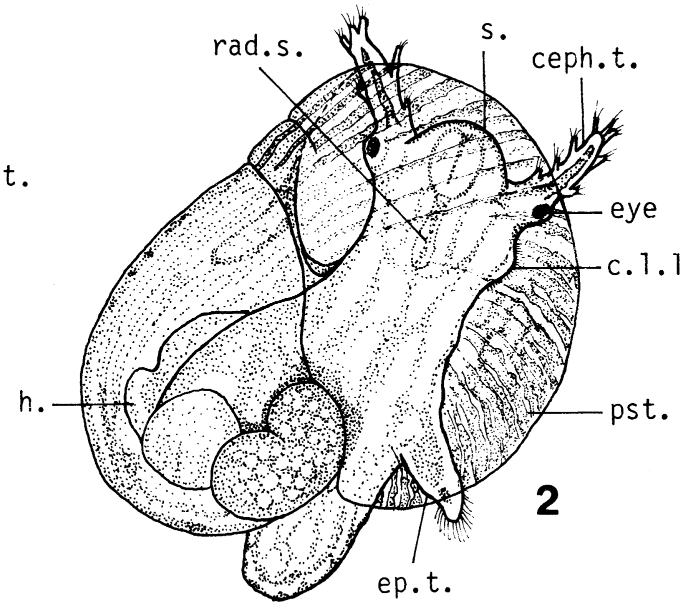

2

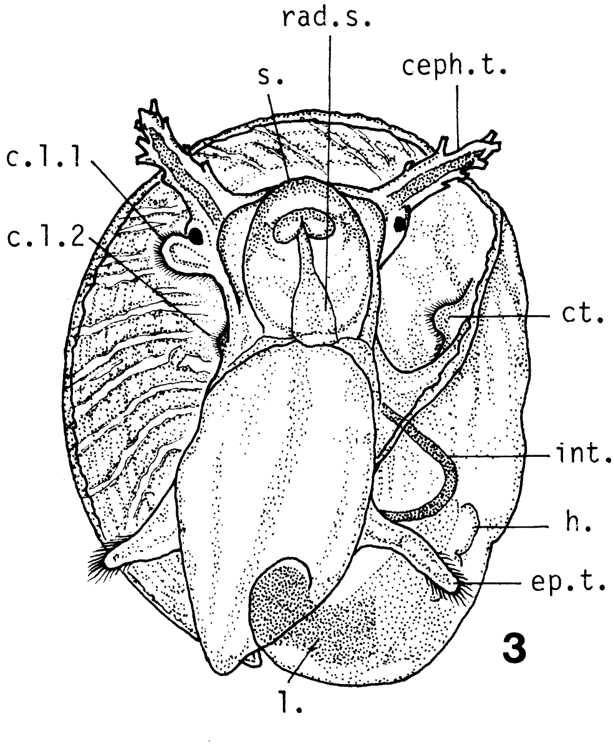

3

4

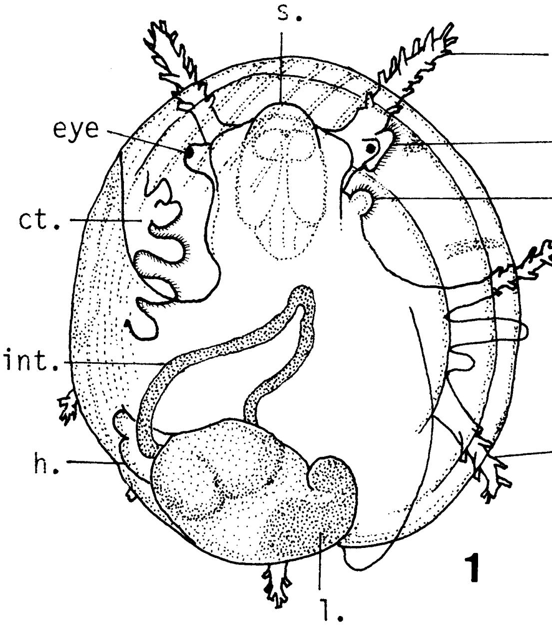
s.
eye
ct.
int.
h.
l.
ceph.t.
c.l.1
c.l.2
ep.t.

1

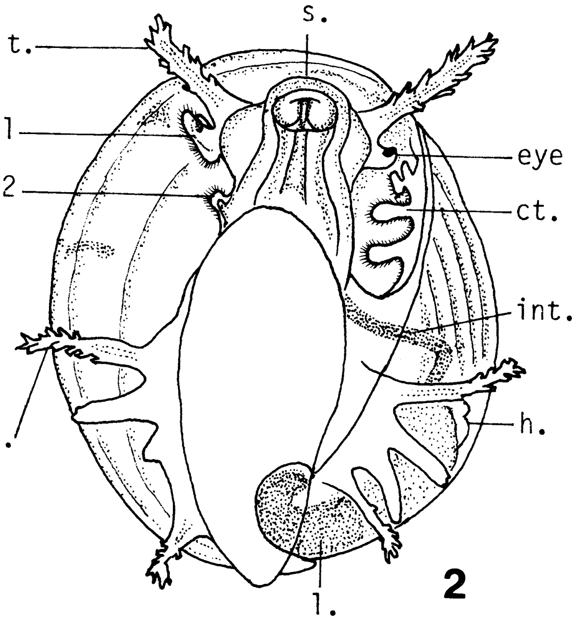
s.
eye
ct.
int.
h.
l.

2

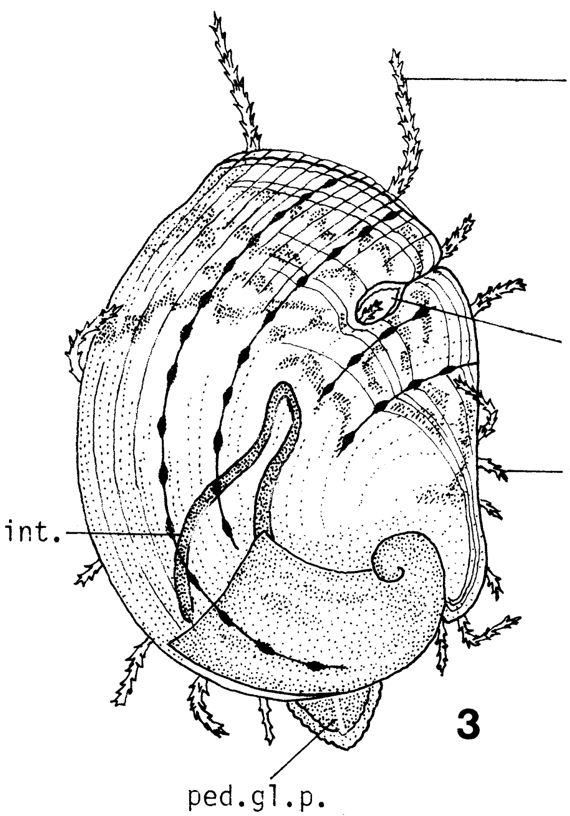
ceph.t.
resp.p.
ep.t.
int.
ped.gl.p.

3

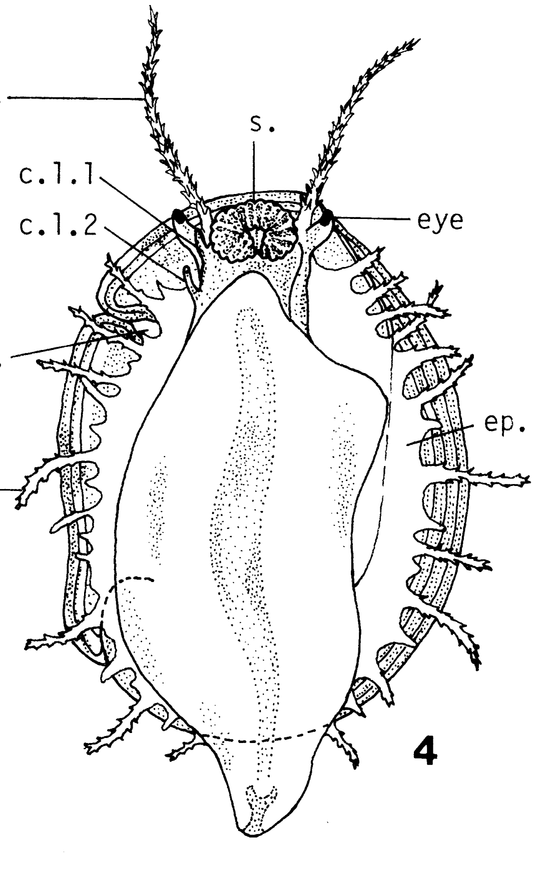
s.
c.l.1
c.l.2
eye
ep.

4

PLATE V

1

2

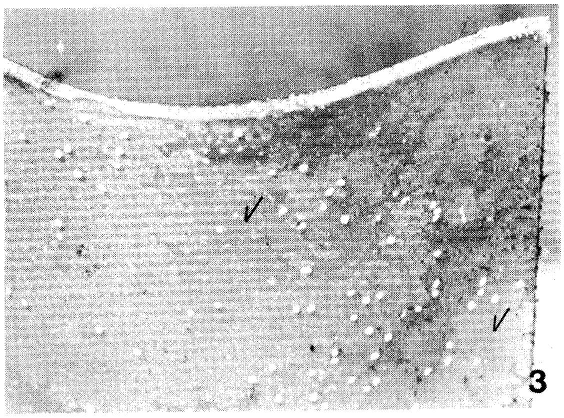

3

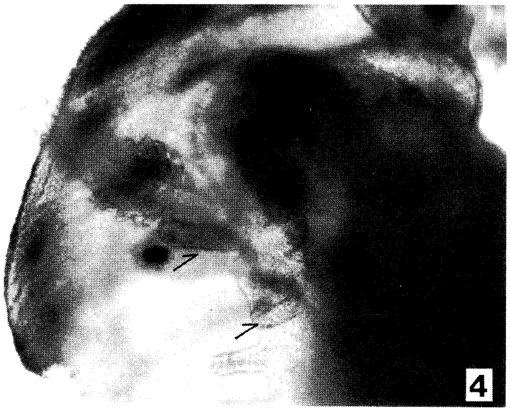

4

5

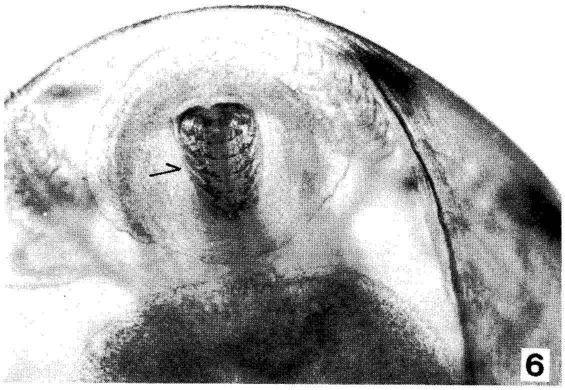

6

PLATE VI

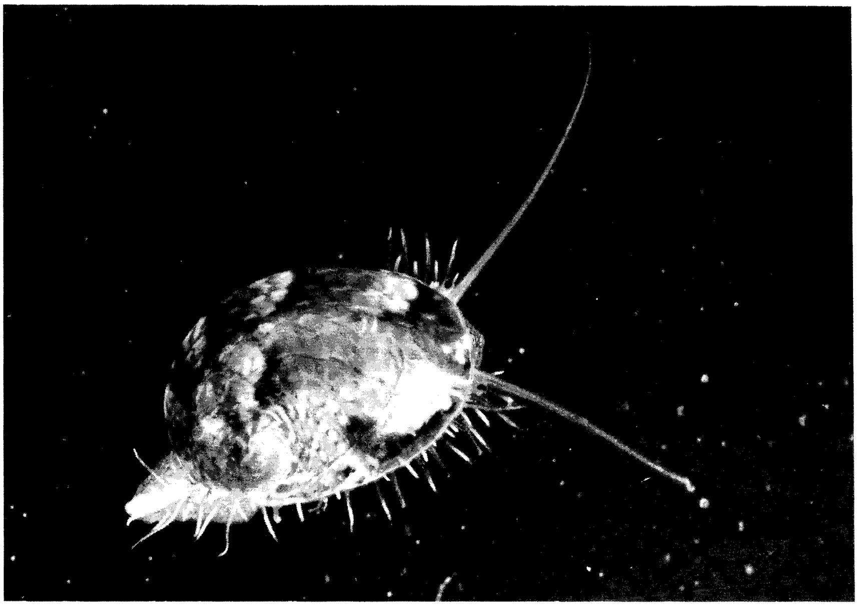

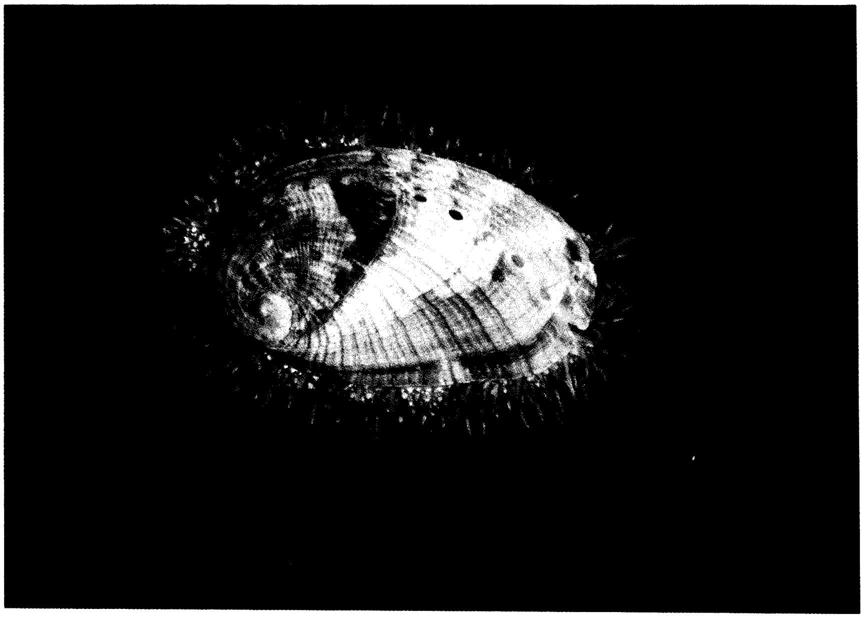

La mer (Bulletin de la Société franco-japonaise d'océanographie)
Tome 16, N° 3, pp. 147 à 161, Août 1978

Effect of the Approximation to the Equation of State for Sea Water on the Model General Circulation*

Kenzo TAKANO**

Abstract: In place of the Knudsen formula, simpler approximate equations of state are used for computing the density of sea water in the numerical models of the ocean circulation. In order to understand how the approximation to the equation of state affects a model general circulation driven by a thermal forcing, we carry out numerical experiments with two different equations of state. One is a linear function of the temperature with a constant coefficient of thermal expansion of 2.5×10^{-4}°C^{-1}, and the other is an equation by FRIEDRICH and LEVITUS giving the density as a little more complicated function of the temperature, pressure and salinity. The salinity is assumed to be 35 ‰ everywhere. The former suppresses a cyclonic gyre at high latitude upper layers to develop a large anticyclonic gyre all over the upper layers, whereas it overestimates the horizontal and vertical circulation and the meridional heat transport, considerably increases high latitude surface temperatures and a little increases tropical surface temperatures.

1. Introduction

The Knudsen formula for computing the the density of sea water from hydrographic data is so complicated that simpler approximate polynomial formulas have been used in the numerical models of the ocean circulation so far developed.

The simplest one gives the density ρ as a linear function of the temperature T with a coefficient of thermal expansion α and a constant ρ_0 as

$$\rho=\rho_0(1-\alpha T). \qquad (1)$$

Not a few models used this formula for its simplicity, though its accuracy is poor when α is assumed to be constant. A value of 2.0 to 2.5×10^{-4}°C^{-1} is usually assigned to α. However, the coefficient of thermal expansion of sea water decreases with decreasing temperatures and decreasing salinities except at low salinities and low temperatures. For instance, for surface waters of 35 ‰ it takes a value of 3×10^{-4}°C^{-1} at $T=25$°C, 2.5×10^{-4}°C^{-1} at $T=19$°C and 1×10^{-4}°C^{-1} at $T=4$°C. Since the effect of the pressure is relatively small, Formula (1) with $\alpha=2.0$ to 2.5×10^{-4}°C^{-1} underestimates the density change by the temperature change for warm water in tropical surface layers and greatly overetimates it for cold water at high latitudes and in deep layers.

The density field is closely linked with the pressure field, which in turn is closely linked with the velocity field. Therefore, Formula (1) may significantly distort the numerical solution of the general circulation in a large ocean where the temperature varies over a wide range. The present study shows, by several examples, to what extent the approximation to the equation of state affects the model general circulation.

2. Model

The model ocean extends from the equator to 70°N and over 48° in longitude. The depth is 4000 m everywhere. The horizontal grid size is 2° in both longitude and latitude. The momentum advection has no significant effect when such a coarse grid is set up. Thereby, the momentum equations are given by

$$\frac{\partial u}{\partial t}=-\frac{1}{\rho R\cos\varphi}\frac{\partial p}{\partial \lambda}+2\omega v\sin\varphi + A_M\nabla^2 u+\kappa_M\frac{\partial^2 u}{\partial z^2},$$

* Received June 10, 1978
** Rikagaku Kenkyusho, Wako-shi, Saitama-ken 351, Japan

$$\frac{\partial v}{\partial t}=-\frac{1}{\rho R}\frac{\partial p}{\partial \varphi}-2\omega u\sin\varphi$$
$$+A_M\nabla^2 v+\kappa_M\frac{\partial^2 v}{\partial z^2},$$
$$0=-\frac{1}{\rho}\frac{\partial p}{\partial z}-g,$$
$$\nabla^2=\frac{1}{R^2\cos\varphi}\left\{\frac{1}{\cos\varphi}\frac{\partial^2}{\partial\lambda^2}+\frac{\partial}{\partial\varphi}\left(\cos\varphi\frac{\partial}{\partial\varphi}\right)\right\},$$

where λ is the longitude, φ the latitude, z the vertical coordinate positive upward, t the time, u, v and w are the eastward, northward and upward component of the velocity, p the pressure, R and ω are the radius and angular velocity of the earth, g is the acceleration of gravity, A_M the coefficient of horizontal eddy diffusivity and κ_M the coefficient of vertical eddy diffusivity.

The equation of continuity is

$$\frac{1}{R\cos\varphi}\left\{\frac{\partial u}{\partial\lambda}+\frac{\partial}{\partial\varphi}(v\cos\varphi)\right\}+\frac{\partial w}{\partial z}=0. \quad (2)$$

The equation for the temperature is given by

$$\frac{\partial T}{\partial t}=-\frac{1}{R\cos\varphi}\left\{\frac{\partial}{\partial\lambda}(uT)+\frac{\partial}{\partial\varphi}(vT\cos\varphi)\right\}$$
$$-\frac{\partial}{\partial z}(wT)+A_H\nabla^2 T+\frac{\kappa_H}{\delta}\frac{\partial^2 T}{\partial z^2},$$

where A_H and κ_H are the coefficients of eddy diffusivity for heat.

The coefficient δ is defined by

$$\delta=\begin{cases}1\\0\end{cases}\quad\text{for}\quad\frac{\partial T}{\partial z}\begin{matrix}>\\ \leqq\end{matrix}0,$$

which parameterizes the vertical mixing process in such a way that strong vertical mixing restores a neutral stratification whenever the vertical stratification becomes unstable.

Three cases are dealt with. Formula (1) is applied to Cases 1 and 3, and a formula by FRIEDRICH and LEVITUS (1973), hereafter referred to as F&L, to Case 2. Of these two formulas the latter, giving the density variable with temperature, pressure and salinity, is much more accurate than the former which ignores the variation of the coefficient of thermal expansion with temperature. Because the salinity is excluded in the present study, it is made 35‰ everywhere in Case 2.

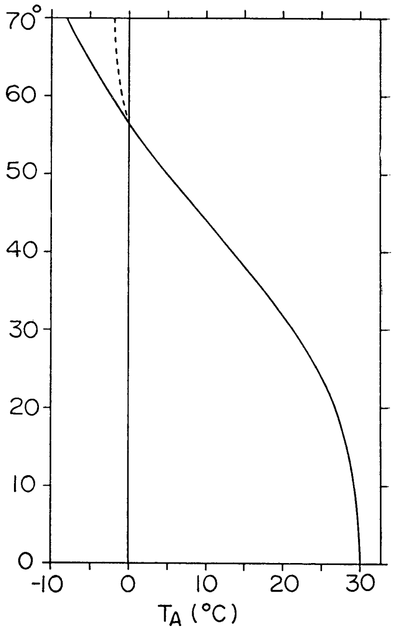

Fig. 1. Reference atmospheric temperature T_A. Solid line for Case 1 and broken line for Cases 2 and 3.

The boundary conditions at the surface are

$$w=0, \quad (3)$$

$$\kappa_H\frac{\partial T}{\partial z}=d(T_A-T_S), \quad (4)$$

$$\kappa_M\frac{\partial}{\partial z}(u,v)=(0,0). \quad (5)$$

The surface heat flux is assumed to be proportional to the difference between the calculated surface temperature T_S and a prescribed reference atmospheric temperature T_A which depends on the latitude only. The constant d is somewhat arbitrary. It is taken here as 50 cal cm^{-2} day^{-1}. Figure 1 shows T_A for Case 1 by a solid line and T_A for Cases 2 and 3 by a broken line.

So far as the formulation is concerned, Cases 1 and 3 are identical with each other except for T_A. Only at high latitudes north of 56°N it is higher in Cases 2 and 3 than in Case 1. The reason why T_A is modified in Cases 2 and 3 so as to weaken the surface cooling at high latitudes is as follows. In the case where

Formula F&L is used, the density increase by the temperature decrease is very small at low temperatures. It takes, therefore, long time for the high latitude surface water to be, by surface cooling, dense enough to sink from the surface to deeper layers. The surface temperature decreases and reaches the freezing point ($-1.8°C$), if the same T_A as in Case 1 is used in Case 2. Obviously the reference atmospheric temperature used in Case 1 leads to an excessive surface cooling, when the density increase by the temperature decrease is correctly calculated by Formula F&L. In other words, when the density is calculated by Formula (1), the density increase due to the temperature decrease is so large at low temperatures that the high latitude surface water can not remain at the surface for a longtime, and readily sinks to deeper layers before its temperature does drop correctly. The broken line in Fig. 1 is subjectively drawn in such a way that the surface temperature does not reach the freezing point. To be compared with Case 2, supplemented is an additional case, Case 3, where Formula (1) is used together with the same T_A as in Case 2.

No wind stress is applied to the ocean surface in the three cases, which might be helpful to make clear the effect of the degree of approximation to the equation of state.

There is no heat flux through the bottom and the lateral boundary. There is no friction along the bottom and the southern boundary, no slip along the western, northern and eastern boundary. Symmetry is assumed with respect to the southern boundary.

The grid is staggered. The u and v points are 1° distant in both longitude and latitude from the T, p and w points. The lateral boundary is defined by T, p and w points.

In the vertical, five levels are set up to calculate u, v and T at depths of 20, 120, 640, 1280 and 2760 m, and w at depths of 70, 380, 960 and 2020 m.

The finite differencing is not described here, because it is almost the same as that detailed in another paper (TAKANO, 1974).

Principal numerical parameters are as follows:

$$\alpha=2.5\times10^{-4}{}^{\circ}C^{-1},$$
$$A_M=2\times10^{8}\ cm^2\ sec^{-1},$$
$$A_H=2.5\times10^{7}\ cm^2\ sec^{-1},$$
$$\kappa_M=\kappa_H=1.5\ cm^2\ sec^{-1},$$

time step=8 hours.

The time integration is fundamentally leapfrog with the Matsuno's backward differencing applied every ten time steps. Case 1 starts from an initial state where the temperature varies with depth and latitude. Then, the time integration is forwarded over 104.1 years. Cases 2 and 3 start from the final state of Case 1. Case 2 runs over 30.4 years. Case 3 runs over 16.3 years. A period of integration of tens of years is not long enough to get a steady state in the whole ocean basin. A secular variation is still persistent at the last stage of the time integration. At the end of the integration, the temperature averaged over the whole ocean basin is decreasing at a rate of 0.015°C $year^{-1}$ in Case 1 and of 0.004°C $year^{-1}$ in Case 3, and is increasing at a rate of 0.018°C $year^{-1}$ in Case 2. However, an almost steady state is reached in each case. There is no short time scale fluctuation because of the large coefficients of eddy diffusivity.

3. Velocity field

Case 1. The horizontal velocities at depths of 20, 640 and 2760 m are shown in Figs. 2 to 4. This case is somewhat similar to Case 1 in a paper by BRYAN and COX (1967). The ocean shape, the grid size and the coefficients of eddy diffusivity are not identical with each other. The temperature in their study is an "apparent temperature" including the salinity implicitly. In addition, it is the apparent temperature that is prescribed at the ocean surface as a thermal boundary condition, while the thermal condition at the ocean surface is given here in terms of the surface heat flux calculated by (4). There are no significant differences between the two solutions, however. A single large anticyclonic gyre spreads almost all over the surface. A western boundary current flows northward all along the western boundary. It gradually widens downstream.

The currents at 120m are a little weaker. The maximum speed of the western boundary current decreases from 29.3cm sec^{-1} at 20m to 26.9cm sec^{-1} at 120m. The current pattern does

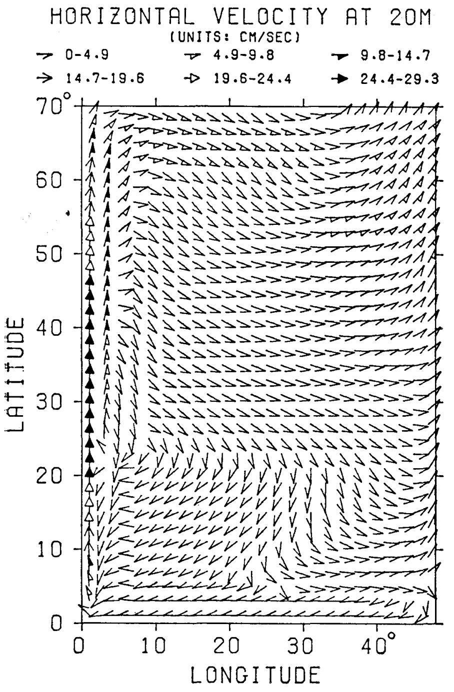

Fig. 2. Horizontal velocity field at a depth of 20 m in Case 1.

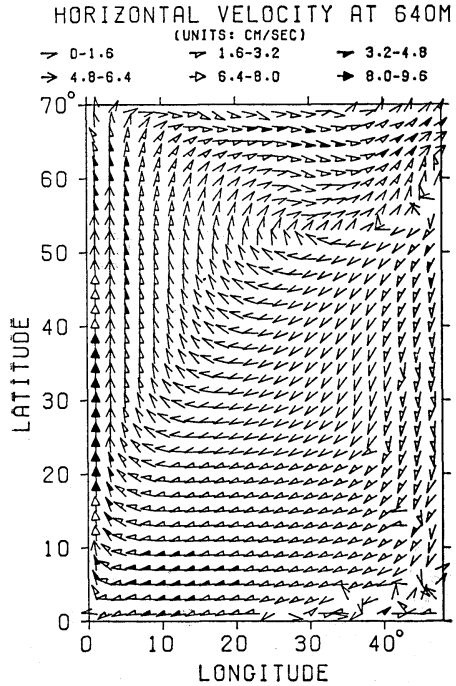

Fig. 3. Horizontal velocity field at a depth of 640 m in Case 1.

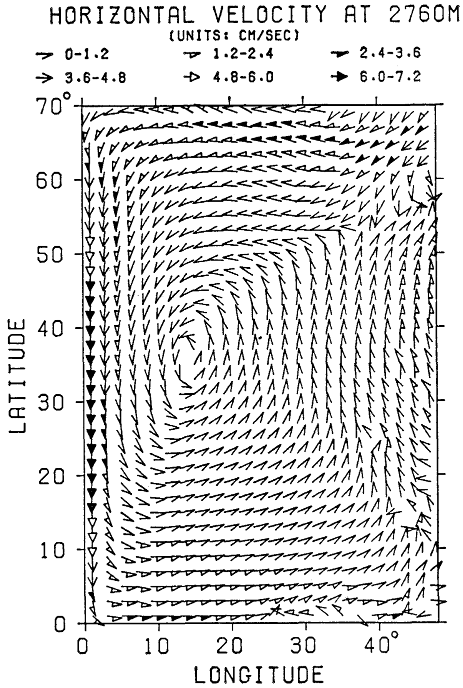

Fig. 4. Horizontal velocity field at a depth of 2760 m in Case 1.

not change from that in Fig. 2 except in the south-eastern region of the ocean basin. A weak, broad eastern boundary current flows southward south of 35°N. The currents are mostly westward between the equator and 20°N except in the eastern and western boundary region. The southern border of the eastward currents at middle and high latitudes goes up north by 6°. The anticyclonic gyre is, as it were, a little pushed northward.

The western boundary current is much broader at 640m than at upper layers. It spreads over almost half the zonal extent of the ocean basin at high latitudes. The anti-cyclonic gyre is better organized and further pushed northward. Its center is located around 35°N in the eastern boundary region.

The vertical integral of the horizontal velocity from the bottom to the surface vanishes everywhere, because there are no wind stress, no momentum advection, no bottom friction, no depth change. Hence, the currents at upper layers are compensated by the currents at lower layers. At 1280m, the equatorial current flows still westward as it does at the upper layers, but the western boundary current changes its direction and flows southward. The current direction is almost reversed at low and middle latitudes. Going further north, the anticyclonic gyre is centered around 60°N to the east of 40° in longitudc. A cyclonic gyre is emerging to the south of this main gyre.

At 2760m a single large cyclonic gyre is well developed with a strong southward current along the western boundary, which is much broader than the northward boundary current at the surface layer. The equatorial current flows eastward. There is no anticyclonic gyre any longer at high latitudes.

Case 2. The velocity field is strikingly different from that in Case 1. Figure 5 shows the velocity distribution at 20m. The anticyclonic gyre prevailing at the surface layer in Case 1 is, roughly speaking, shifted southward by about 15° in latitude. It is between 13°N and 31°N that the western boundary current is fastest, while it is between 19°N and 45°N in Case 1. The maximum speed considerably decreases from

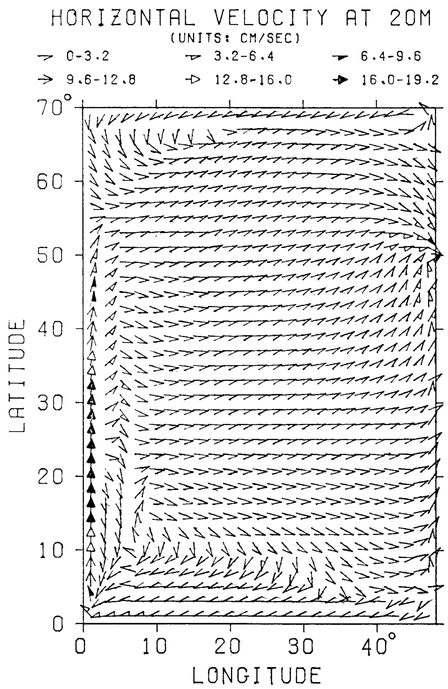

Fig. 5. Horizontal velocity field at a depth of 20 m in Case 2.

29.3cm sec^{-1} in Case 1 to 19.2cm sec^{-1} in Case 2. North of 55°N there appears a cyclonic gyre with a broad, weak western boundary current flowing southward. In contrast with a single gyre circulation in Case 1, a double gyre circulation, though the cyclonic one is much weaker, is thus driven provided that Formula F & L is used instead of (1). The effect of Formula F & L can be interpreted as an additional heating of the high latitude surface applied to Case 1, which upsets the overestimate of the density increase by the temperature decrease resulting from Formula (1). As is mentioned above, the coefficient of thermal expansion, 2.5×10^{-4}°C^{-1}, holds good around a temperature of 20°C only. A high latitude additional heating gives rise to a cyclonic gyre with a western boundary current flowing southward. The appearence of the cyclonic gyre is readily understood in this way, although the velocity field in Case 2 is not merely a linear superposition of the velocity field produced by this additional heating upon the velocity field obtained in Case 1.

Formula F & L brings about an additional heating to the equatorial region in Case 1, too, so as to make up the density decrease by the temperature increase which is underestimated by Formula (1). However, when α is taken as 2.5×10^{-4}°C^{-1}, the resulting error in the equatorial region is much smaller than that in the high latitude region. This is the reason why Formula (1) is not so wrong there as at high latitudes.

The currents flow eastward with very weak meridional component in the central and eastern region between 10°N and 20°N. In Case 1 the zonal component is not so pronounced there: the currents flow southwest in the western half, south in the central region and southeast in the eastern region.

The motion is slightly weaker at 120m. The maximum speed of the western boundary current decreases from 19.2cm sec^{-1} at 20m to 15.9cm sec^{-1} at 120m. The current pattern is close to each other except in the equatorial region. At 20m the westward current north of the equator is about 8° wide in the west and about 4° wide in the east. At 120m it is

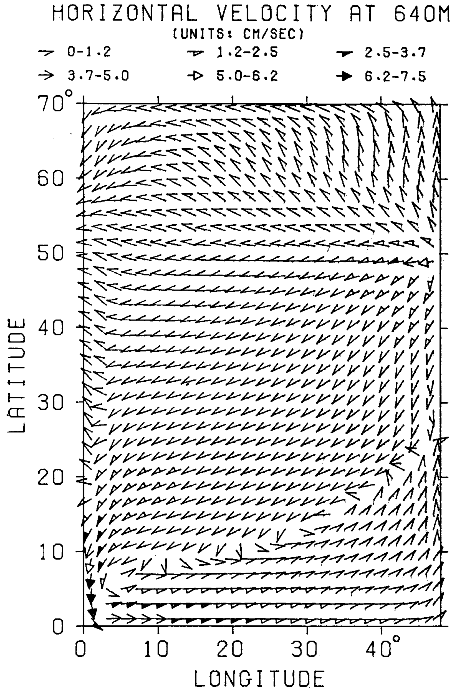

Fig. 6. Horizontal velocity field at a depth of 640 m in Case 2.

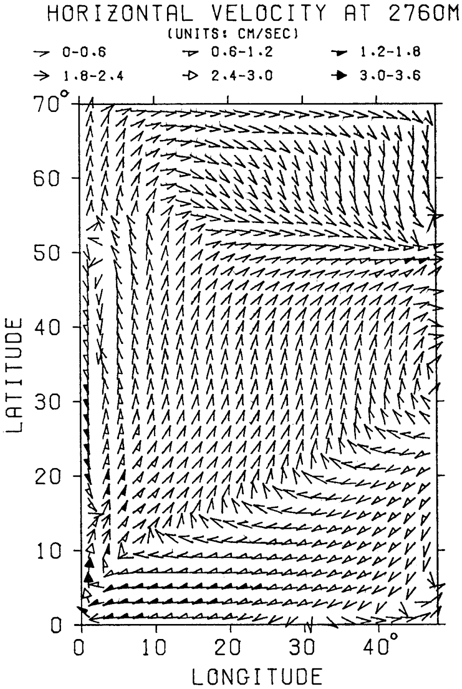

Fig. 7. Horizontal velocity field at a depth of 2760 m in Case 2.

about 22° wide in the west and about 26° wide in the east except in the boundary region, indicating that the center of the anticyclonic gyre is located between 22°N and 26°N, far north of its center at a depth of 20m located between 4°N and 8°N. The northern border of the gyre does not go up. It is still around 55°N.

At 640m there is no western boundary current except south of about 15°N as is shown in Fig. 6. The circulation is cyclonic rather than anti-cyclonic, with eastward currents between 0° and 10°N and westward currents at higher latitudes. It might be remarked that Case 1 shows a well organized anticyclonic gyre: there are westward currents at low and middle latitudes and eastward currents at high latitudes (Fig. 3).

The northward current along the western boundary and the westward equatorial current are much shallower in Case 2 than in Case 1.

The southward current along the western boundary develops northward with depth. At 1280m it starts from 55°N. No northward

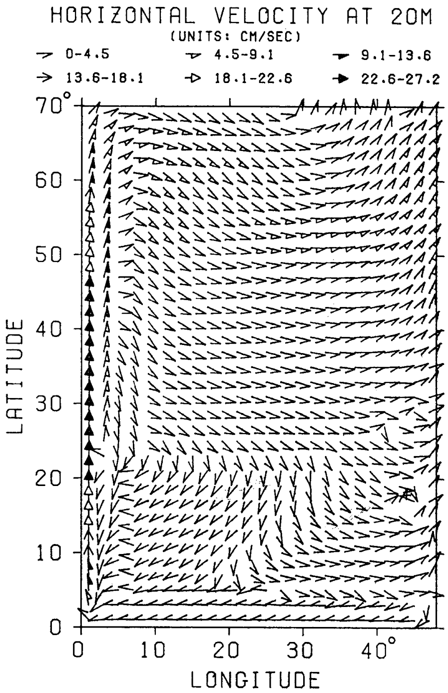

Fig. 8. Horizontal velocity field at a depth of 20 m in Case 3.

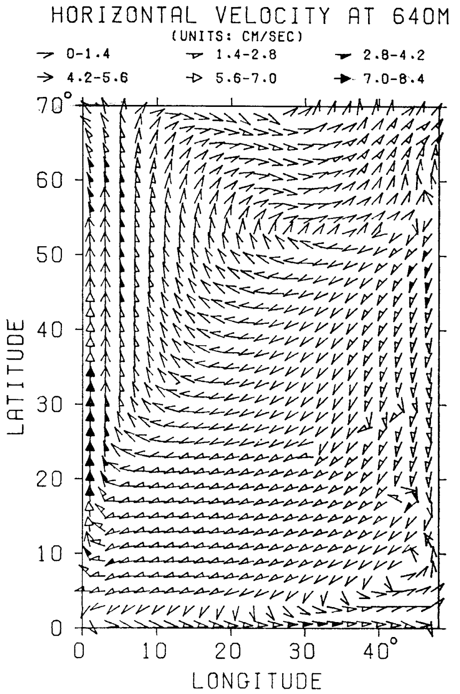

Fig. 9. Horizontal velocity field at a depth of 640 m in Case 3.

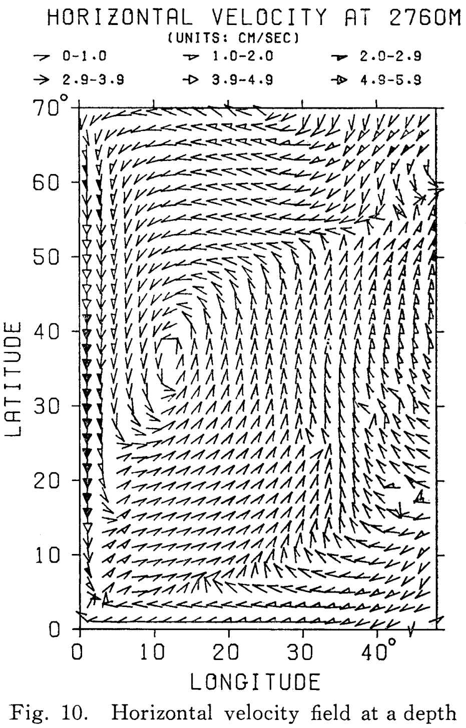

Fig. 10. Horizontal velocity field at a depth of 2760 m in Case 3.

boundary current is present as yet north of 55°N. The equatorial current flows again westward in the eastern half at 1°N.

Figure 7 gives the velocity field at 2760m. The currents are mostly northward at middle latitudes except near the western boundary, where a relatively strong current, though not faster than $1.8\,\mathrm{cm\,sec^{-1}}$, flows southward. To the south of this southward current there is a strong northward current, and to the north there is a weak northward current. This contrasts strikingly with the pattern in Case 1. Common features between the two are only the southward current along the western boundary at middle latitudes and the northward currents in mid-ocean at middle latitudes.

Case 3. The horizontal velocities at three levels are shown in Figs. 8 to 10. The pattern at 20 m resembles closely the pattern in Case 1, although the motion is slightly weaker due to the weaker cooling by the higher T_A in the northern boundary region. The pattern at 640m is, however, a little different from each other in the equatorial region: the currents flow eastward all along a parallel of 1°N as in Case 2, indicating that the westward equatorial current in surface layers is shallower in Case 3 than in Case 1. Except for the equatorial current at 1°N, the difference between Cases 2 and 3 is no less than the difference between Cases 2 and 1.

Contrary to Case 1, the western boundary current at 1280m starts from the northern boundary and flows south to the equator, and then turns to the east. This also suggests that the surface western boundary current flowing northward should be shallower in Case 3 than in Case 1. In this regard, the result in Case 3 is closer to the result in Case 2 than to the result in Case 1. The currents are eastward in the equatorial region between 0° and 10°N, whereas they are mostly westward in Case 1 and eastward in Case 2.

The pattern at 2760m agrees fairly well with the pattern in Case 1 except for the southeast half of the tropical region where the currents are mostly westward, opposite to Case 1.

4. Temperature field

Case 1. Figure 11 shows the temperature field at a depth of 120m. Related to the northward strong current, isotherms are strikingly pushed northward near the western boundary. They are slightly pushed northward near the eastern boundary where the currents are northward north of 39°N, southward south of 39°N at this depth, and northward everywhere at 20m.

The isotherm pattern at 20m is alike, but the northward pushing is much less pronounced near the western boundary, because the surface temperature is controlled to a greater extent by the prescribed reference atmospheric temperature which does not vary with longitude.

The temperature at 1280m is shown in Fig. 12. A warm tongue-like core extends from the eastern boundary around 60°N to the west and then to the southwest. A cold water mass, absent at a depth of 640m, whose lowest temperature is 1.3°C on the eastern boundary, extends to the south of the warm core. This cold water mass is further enlarged at 2760m. A sharp thermal gradient by the eastern boundary between the warm and cold water mass, located around 59°N at 2760m, about 7° north of its location at 1280m, is closely related to the transition of the vertical component of the velocity from the southern upwelling to the northern sinking in the eastern boundary region.

Case 2. Figure 13 gives the temperature field at

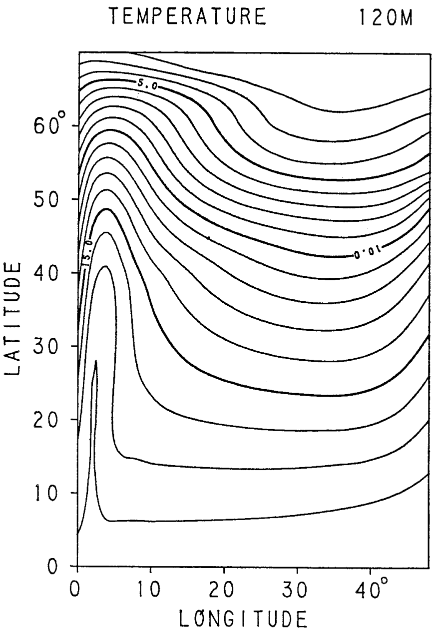

Fig. 11. Temperature field at a depth of 120 m in Case 1.

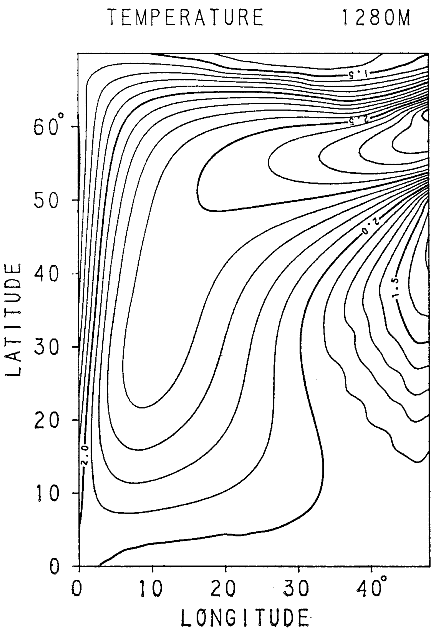

Fig. 12. Temperature field at a depth of 1280 m in Case 1.

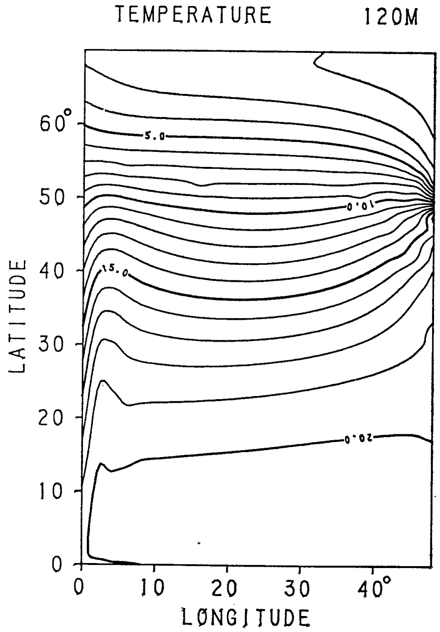

Fig. 13. Temperature field at a depth of 120 m in Case 2.

120m in Case 2. Corresponding to the wane of the northward current and to the presence of the southward current north of 55°N, the northward pushing of isotherms is much less pronounced than in Case 1.

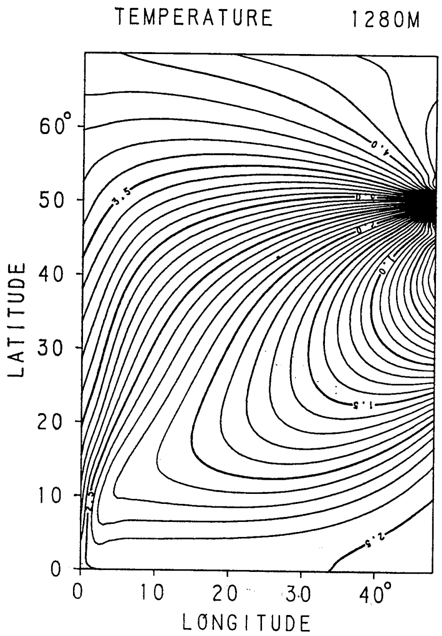

Fig. 14. Temperature field at a depth of 1280 m in Case 2.

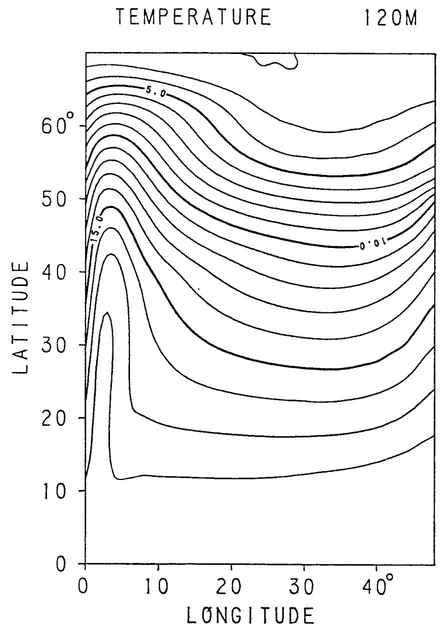

Fig. 15. Temperature field at a depth of 120 m in Case 3.

What is peculiar to the temperature fields at the five levels in Case 2 is that isotherms are crowded into a small area around 50°N in the eastern boundary region located at the border between the anticyclonic and cyclonic gyre. This area coincides with strong convergence at depths of 20, 120 and 2760m, and with strong divergence at depths of 640 and 1280m. This peculiarity is well brought in Fig. 14. The maximum of the vertical component of the velocity at each level is found there: -1.07×10^{-2}cm sec^{-1} at 70m, -3.96×10^{-2}cm sec^{-1} at 380m, -2.45×10^{-2}cm sec^{-1} at 960m and 3.14×10^{-2}cm sec^{-1} at 2020m. Crowding of isotherms is seen in Case 1, too, but only at the lower three levels.

Case 3. The isotherm patterns at the five levels are not very different from those in Cases 1 and 2. For instance, the temperature field at 120 m shown in Fig. 15 is similar to that in Case 1. The northernmost region is slightly warmer because of weaker cooling due to the higher T_A.

The temperature ranges at the upper two levels in the three cases are given in Table 1.

Table 1. Temperature ranges (°C) at the upper two levels.

	Case 1	Case 2	Case 3
20 m	1.4 to 27.4	−1.0 to 27.8	2.0 to 27.5
120 m	1.4 to 18.4	1.6 to 20.3	2.0 to 19.5

The same T_A is applied to Cases 2 and 3, but the lowest surface temperature is lower by 3°C in Case 2 than in Case 3, and the highest surface temperature is slightly higher in Case 2 than in Case 3, because the accuracy of Formula (1) is poorer at high latitudes than at low latitudes as mentioned earlier. Compared with Case 1, both the highest and lowest temperature in Case 3 are a little higher at 20 m and 120 m as a result of weaker cooling at high latitudes. The temperature averaged over the whole ocean basin is 3.38°C in Case 1, 4.02°C in Case 2 and 3.32°C in Case 3.

5. Total meridional circulation

Integrating Equation of continuity (2) from

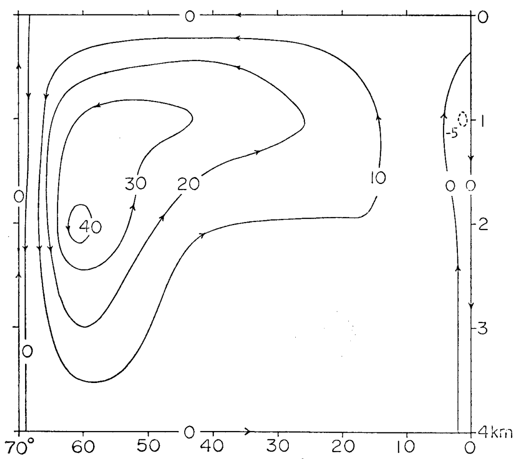

Fig. 16. Total meridional circulation in Case 1 (units: 10^{12} cm^3 sec^{-1}).

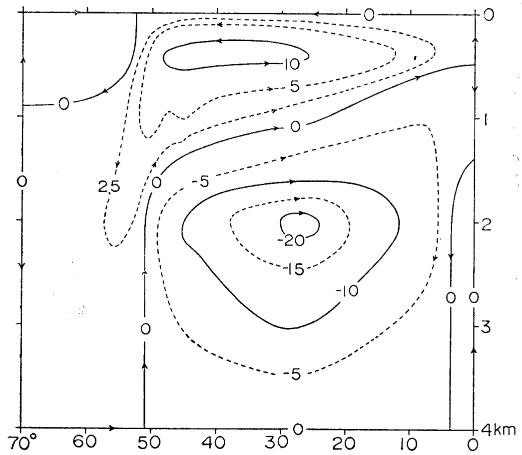

Fig. 17. Total meridional circulation in Case 2 (units: 10^{12} cm^3 sec^{-1}).

the western boundary to the eastern boundary, we have

$$\frac{1}{R}\frac{\partial}{\partial\varphi}\int v\cos\varphi\, d\lambda+\frac{\partial}{\partial z}\int w\cos\varphi\, d\lambda=0\,.$$

This equation permits to introduce the transport stream function Φ for the longitudinal total of the meridional circulation defined by the relations

$$\int vR\cos\varphi\, d\lambda=-\frac{\partial\Phi}{\partial z},$$

$$\int wR\cos\varphi\, d\lambda=\frac{1}{R}\frac{\partial\Phi}{\partial\varphi}.$$

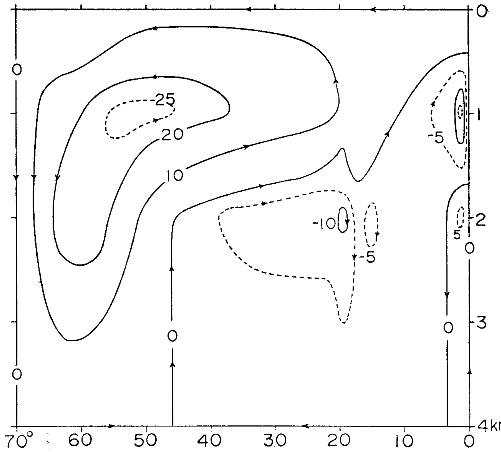

Fig. 18. Total meridional circulation in Case 3 (units: 10^{12} cm^3 sec^{-1}).

Figures 16 to 18 show the total meridional circulation in Cases 1 to 3 in terms of the stream function which is made equal to 0 at the boundary.

Case 1. There appears a large counterclockwise gyre with sinking in the north and weak upwelling in the south, centered at 2020 m, 61°N. The maximum value of the stream function, *i.e.*, the total transport of the meridional circulation is 42.5×10^{12} cm^3 sec^{-1}. In addition to this major gyre, there is a weak clockwise gyre just north of the equator, whose intensity is only 5×10^{12} cm^3 sec^{-1}. The downward transport in deep layers at the equator is mainly due to the downward motion at the eastern region at 960 m and at the western region at 2020 m.

Another minor clockwise gyre is seen close to the northern boundary. Its transport is only 0.3×10^{12} cm^3 sec^{-1}. A strong sinking occurs at the eastern region on the northern boundary, but a weak upwelling in the central region and a fairly strong upwelling in the western region upset the downward transport to make a net weak upward transport along the northern boundary.

The sinking region of the major gyre is much narrower than the upwelling region just as shown by BRYAN and COX (1967). The latitudinal extent of the former is about 8°, while the extent of the latter is about 58°.

The main source of the downward transport is a strong downward motion along the eastern boundary. The maximum downward speed at each level is found there: 1.0×10^{-2} cm sec^{-1} at 70 m, 5.2×10^{-2} cm sec^{-1} at 380 m, 10.3×10^{-2} cm sec^{-1} at 960 m and 14.3×10^{-2} cm sec^{-1} at 2020 m.

Case 2. The pattern changes strikingly. The major counterclockwise gyre in Case 1 shrinks, shallows and shifts southward. Its center is located at 380 m, 39°N. Its northern border around 52°N coincides with the convergence between the anticyclonic and cyclonic gyre mentioned above. Its transport is 12×10^{12} cm^3 sec^{-1} compared with 43×10^{12} cm^3 sec^{-1} in Case 1. The weak northern boundary gyre in Case 1 grows southward into a shallower but larger gyre of 1.4×10^{12} cm^3 sec^{-1}. As in Case 1, the upward transport at the northern boundary region originates mainly from the upwelling in the western boundary region.

At low and middle latitudes below the counterclockwise gyre emerges a large clockwise gyre whose transport is 21×10^{12} cm^3 sec^{-1}, almost twice as large as the transport by the upper counterclockwise gyre.

The downward transport at a depth of 2020 m between 10°N and 27°N results mostly from the sinking at the eastern boundary, whose maximum is 1.7×10^{-2} cm sec^{-1} at 22°N. There is a sinking along the western boundary at these latitudes, too, but it is much weaker except at 10°N to 14°N. This downward transport is lacking in Case 1, where, contrary to Case 2, a strong upward motion is found almost all along the eastern boundary, and the upward motion in mid-ocean is also a little stronger than in Case 2. An upwelling at the eastern boundary gives rise to the upward motion between 27°N and 51°N, though a weak sinking at the western boundary reduces it.

Case 2 runs over 30.4 years only. One may ask oneself, therefore, whether or not the time integration is long enough to get an almost steady state which is capable of meaningful description. In parallel with the present study, another study is done for the circulation driven by not only the surface heat flux but also the surface salinity flux. The time integration is forwarded over 120 years. The resulting meridional circulation pattern does not essentially differ from that in Case 2. A deep clockwise gyre is present below the upper counterclockwise gyre just as in Case 2, indicating that Fig. 17 is not a transition phase far from the steady state to be reached.

Case 3. Although the circulation pattern does not significantly differ from that in Case 1, the main counterclockwise gyre is shallower and weaker: the maximum value of the stream function, 27.3×10^{12} cm^3 sec^{-1}, is found at 960 m, 53°N. The northern sinking region is nearly twice as large as that in Case 1. The maximum speed of the downward motion in each level is found on the eastern boundary as in Case 1, but about half as large as that in Case 1: 0.59×10^{-2} cm sec^{-1} at 70 m, 3.0×10^{-2} cm sec^{-1} at 370 m and 6.0×10^{-2} cm sec^{-1} at 2020 m.

Similar to Case 2, four weak clockwise gyres appear at middle and low latitudes.

The downward motion at 2020 m at low latitudes are mainly due to sinking at the eastern boundary which is as strong as in Case 2 and much stronger than in Case 1. The downward transport at the equator is produced by the sinking all along the equator, while the upwelling is produced by the mid-ocean upwelling, though there is a relatively strong sinking at the western and eastern boundary.

Although T_A is a little higher north of 56°N only than in Case 1, the total meridional circulation is affected to such an extent.

It is only the equation of state that is different from each other between Cases 2 and 3. Compared with Case 2, the counterclockwise gyre is strong, though not so much as in Case 1, whereas the clockwise gyre in deeper layers at middle latitudes is almost half in transport.

6. Total zonal circulation

Integrated with respect to the latitude from the southern boundary to the northern boundary, the equation of continuity becomes

$$\frac{1}{R}\frac{\partial}{\partial\lambda}\int u\,d\varphi+\frac{\partial}{\partial z}\int w\cos\varphi\,d\varphi=0\,.$$

The transport stream function is defined, as a measure of the total zonal circulation, by

$$\int uR\,d\varphi=-\frac{\partial\Phi'}{\partial z},\quad \int wR\,d\varphi=\frac{1}{R\cos\varphi}\frac{\partial\Phi'}{\partial\lambda}$$

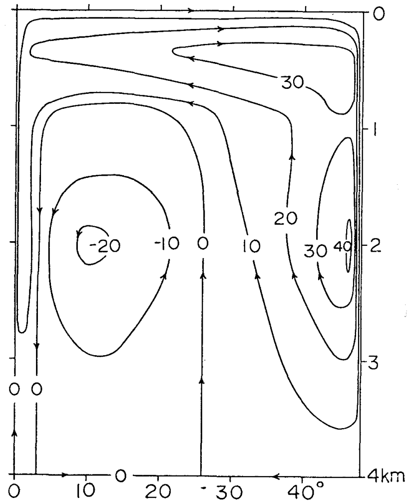

Fig. 19. Total zonal circulation in Case 1 (units: 10^{12} cm^3 sec^{-1}).

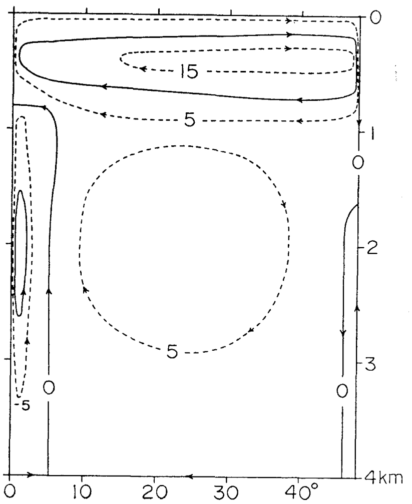

Fig. 20. Total zonal circulation in Case 2 (units: 10^{12} cm^3 sec^{-1}).

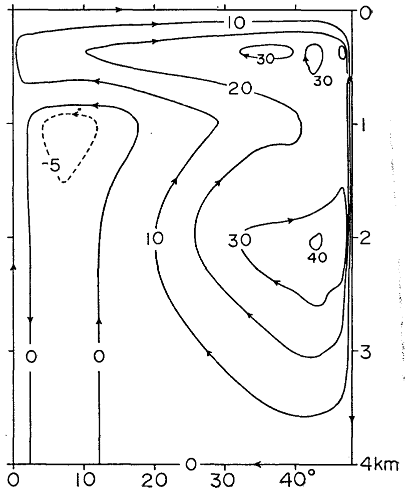

Fig. 21. Total zonal circulation in Case 3 (units: 10^{12} cm^3 sec^{-1}).

Figures 19 to 21 show the total zonal circulation in the three cases in terms of the transport stream function.

Case 1. There are a counterclockwise gyre in the greater part of the eastern half and a clockwise gyre in the remaining region. The latter in turn splits into two small gyres, lower gyre centered at 2020 m, 47° and upper gyre centered at 380 m, 45°. The transport is 41.8×10^{12} cm^3 sec^{-1} and 37.3×10^{12} cm^3 sec^{-1}, respectively. It follows, therefore, that the total zonal circulation is as strong as the total meridional circulation. The strong sinking along the eastern boundary is mainly due to the sinking of cold water from the surface of the northeastern corner. The western boundary region is a strong upwelling region by the upward motion through the length of the western boundary. Its upward transport is 17.5×10^{12} cm^3 sec^{-1} at a depth of 2020 m and 24.2×10^{12} cm^3 sec^{-1} at a depth of 380 m, almost half of the downward transport along the eastern boundary. Alike the total meridional circulation, the total zonal circulation is upward in the greater part of deep layers.

Case 2. The pattern drastically changes. Reflecting the wane of the sinking at high latitudes, particularly in the northeastern corner, the upper clockwise gyre in Case 1 is considerably weakened and confined into upper layers. Its transport is reduced from 37.3×10^{12} cm^3 sec^{-1} in Case 1 to 18.4×10^{12} cm^3 sec^{-1}. The lower clockwise gyre is located at the center and transports 9.8×10^{12} cm^3 sec^{-1}, while in Case 1 it is located near the eastern boundary and is the strongest gyre transporting 40×10^{12} cm^3 sec^{-1}.

The western boundary region splits into two regions: the upper is an upwelling region transporting 13.6×10^{12} cm^3 sec^{-1}, and the lower is a sinking region transporting 14.7×10^{12} cm^3 sec^{-1}, while Case 1 shows an upwelling region extending from the surface down to the bottom.

Case 3. The circulation pattern is close to the pattern in Case 1. Its intensity is less, however. The transports of the three gyres in Case 1 are reduced from 41.8×10^{12} cm^3 sec^{-1}, 37.3×10^{12} cm^3 sec^{-1} and -21.3×10^{12} cm^3 sec^{-1} to 41.2×10^{12} cm^3 sec^{-1}, 33.8×10^{12} cm^3 sec^{-1} and -6.5×10^{12} cm^3 sec^{-1}, respectively.

7. Meridional heat transport

The meridional heat transport across a parallel has three components: transport by the total meridional circulation, transport by the horizontal circulation and transport by the subgrid scale eddy diffusion. The first component is achieved by bringing warm surface waters northward and cold deep waters equatorward. The horizontal circulation yields a net northward heat transport by bringing warm western boundary waters northward and relatively cold waters equatorward in the central and eastern region. The eddy diffusion brings heat from warmer regions to colder regions.

Figure 22 gives the total meridional heat transport in the three cases. Case 1 transports the largest amount of heat, and Case 2 the smallest amount. The meridional heat transport and the surface temperature are interdependent through the surface heat flux which is made proportional to the difference between the surface temperature and the reference atmospheric temperature. The maximum and minimum of the zonal means of the surface temperatures are tabulated in Table 2.

The minimum is found between 68°N and

Table 2. Maximum and minimum of the zonal means of the surface temperatures (°C).

	Case 1	Case 2	Case 3
Max	27.34	27.71	27.74
Min	1.68	−0.86	2.25

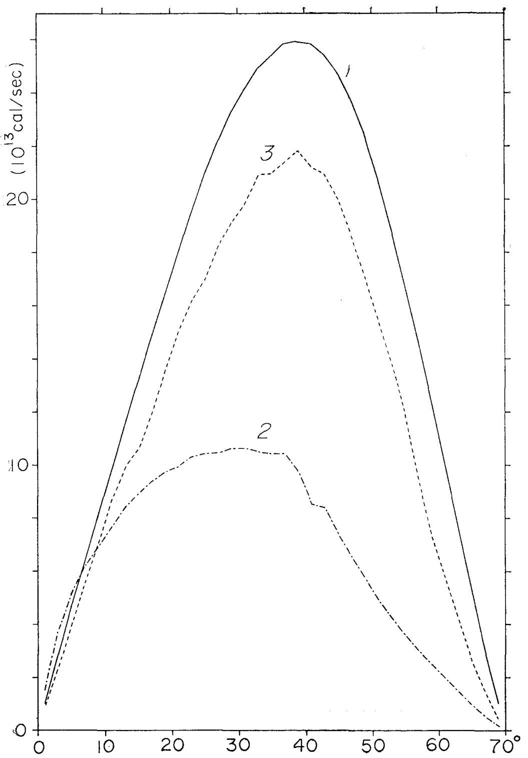

Fig. 22. Total meridional heat transport in Cases 1 to 3. Numbers *1* to *3* written alongside the curves refer to Cases 1 to 3.

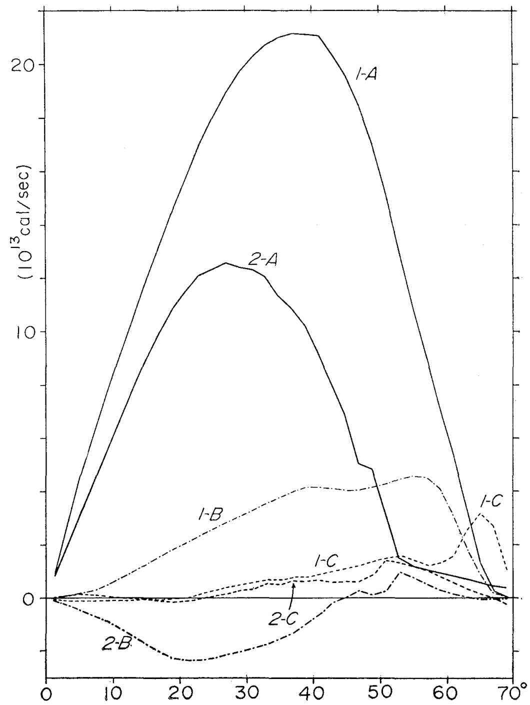

Fig. 23. Three components in Cases 1 and 2. *A*, *B* and *C* denote the transports by the meridional circulation, horizontal circulation and subgrid scale eddy diffusion, respectively.

70°N in every case. The maximum is between 0° and 2°N in Cases 1 and 2, but between 2°N and 4°N in Case 3. On account of these temperatures and the reference atmospheric temperatures at these latitudes, the incoming surface heat flux is largest in Case 1, smallest in Case 2. It is also the case with the outgoing surface heat flux.

Figure 23 gives the three components in Cases 1 and 2. The meridional circulation is of essential importance in any case. The eddy diffusion is considerable at high latitudes only.

Although a larger amount of heat is transported in Case 1 than in Case 3, there is no qualitative difference between the two cases in respect that each component varies with latitude in a quite similar way. About half the difference of the total heat transport between Cases 1 and 3 is accounted for by the difference of the heat transport due to the meridional circulation and the remaining half by the difference of the heat transport due to the horizontal circulation.

However, the decrease of the total heat transport in Case 2 compared with the other two cases is another thing. It is mainly attributed to the decrease of the heat transport by the meridional circulation. The other two components do not decrease much. Another particularity of Case 2 is the role of the horizontal circulation, which transports an amount of heat comparable to that in Case 3. Since the total transport strikingly decreases, its role in the total transport increases relative to the meridional circulation. Moreover, its transport is southward rather than northward. The southward transport south of 45°N is much larger than the northward transport north of 45°N. The transport by the horizontal circulation is northward at any latitude in Case 1, and northward between 0° and 20°N in Case 3.

8. Summary

When a constant coefficient of thermal expansion, 2.5×10^{-4}°C^{-1}, is assumed as in most models of the ocean circulation excluding the salinity, the solution is affected not only at high latitudes but also at low latitudes in various aspects:

(1) High latitude surface temperatures considerably increase.

(2) Equatorial surface temperatures a little decrease.

(3) The double gyre horizontal circulation at upper layers disappears. Instead, a single anticyclonic gyre spreads all over the upper layers. No southward boundary current exists any longer along the high latitude western boundary.

(4) The high latitude sinking is much accelerated. With regard to the total meridional circulation, the deep gyre with sinking at low latitudes and upwelling around 50°N is much decelerated. Too a deep convection penetrates into bottom layers at high latitudes.

(5) The surface western boundary current, equatorial current and other currents become deeper.

(6) The meridional heat transport is spurred thereby. The role of the horizontal circulation decreases relative to the role of the meridional circulation.

(7) Along the western boundary the total zonal circulation shows no deep sinking, although there is still an upwelling in upper layers.

(8) The circulation, either horizontal or vertical, becomes too active.

Neither wind stress nor surface salinity flux comes into play in the present study. Hence, comparison with the observed circulation is out of the scope. A separate paper deals with the change which they bring to the thermal circulation as obtained in Case 2.

The grid used here is not fine enough to resolve the mesoscale eddies whose presence is recently revealed. Although the interaction between the large scale circulation as studied here and the mesoscale eddies is not yet well understood, the approximation to the equation of state should have some effect on the eddy dynamics. Formula (1) is used in almost all the eddy resolved general circulation models so far developed. We carried out a series of numerical experiments by use of Formula F & L and a fine grid in order to have insight into the effect of the degree of the approximation to the equation of state upon the eddy dynamics. A next paper is concerned with the wax of the

eddy activity resulting from Formula (1).

References

BRYAN, K. and M. D. COX (1967): A numerical investigation of the oceanic general circulation. Tellus, **19**, 54–80.

FRIEDRICH, H. and S. LEVITUS (1972): An approximation to the equation of state for sea water, suitable for numerical ocean models. J. Phys. Oceanog., **2**, 514–517.

TAKANO, K. (1974): A general circulation model for the world ocean. Tech. Rept. No. 8, Num. Simul. Weather and Climate, Dept. Meteorol., UCLA, 46 pp.

状態方程式の近似の度合が海洋大循環の数値解に及ぼす影響

高　野　健　三

要旨: 海洋大循環の数値研究では，海水の密度を計算する際に Knudsen の式のかわりに，もっとかんたんな近似多項式を使うのがふつうである。近似の度合が解に及ぼす影響を調べるため，2つの近似式を使って結果をくらべる。大循環は熱だけで駆動される。海水の密度は，第一の近似式では水温の一次関数であるが，第二の近似式では水温と圧力のやや複雑な関数（FRIEDRICH と LEVITUS の式で塩分を一定（35‰）とおいたもの）である。前者では海水の熱膨脹係数は水温や圧力とは関係なく一定となる。この一定値を 2.5×10^{-4}°C^{-1} とする。近似精度は後者のほうがずっと高い。第一の式を使うと，(1) 高緯度の表面水温はいちじるしく上昇し，(2) 赤道海域の表面水温はやや低下し，(3) 低緯度から高緯度へ運ばれる熱量は大きくなり，(4) 高緯度表層の反時計まわりの循環は消えて，ただ一つの時計まわりの循環が表層全部をおおい，(5) 表層海流は一般に深くなり，(6) 子午面鉛直循環はいちじるしく強くなり，(7) 水平循環も強くなる。というわけで，水温の変化幅が広い場合に対しては精度の悪い近似式を使うことは好ましくない。

La mer (Bulletin de la Société franco-japonaise d'océanographie)
Tome 16, N° 3, pp. 162 à 164, Août 1978

日仏海洋学会賞受賞記念講演

おきあみ類をめぐる生物生態に関する研究*

根　本　敬　久**

Recherche écologique d'être vivant relatif aux euphausiacés

Takahisa NEMOTO**

この研究は，私が鯨類研究所および東京大学海洋研究所において続けてきました，動物プランクトン，マイクロネクトンの生態とその捕食者の生態に関する研究の一部として行なわれたものであります。

おきあみ類は現在86種が世界の海洋から報告されています。古くは，1830年代におきあみの一種 *Thysanopoda tricuspidata* が Milne-Edwards により報告されていますが，その後この種に関する研究はむしろ諸外国において進められてきたと考えられます。日本においては，ようやく第二次大戦後になって組織的な研究が始められたと言って良いでしょう。しかし，外洋域のおきあみ類の分布特性や生態に関する広範囲な研究は殆んど行なわれていなかったと言えます。おきあみ類の大型種は，ネットに対する逃避等により極めて採集されにくいため，充分な研究が進められなかったということも一つの理由でしょう。

捕食者として重要なひげ鯨類の餌料として出現したおきあみ類の分布状態を整理した結果，南北両極海域のおきあみ類の分布について新しい知見が得られました。即ち，北太平洋北部海域においては，*Euphausia pacifica*, *Thysanoessa raschii*, *T. inermis*, *T. longipes*, *T. spinifera*, *T. inspinata* の6種が出現します。その分布と現場水温，塩分および海の深度の組合せで出現域を区分しますと，低温低鹹域に出現する *T. raschii* は他の *Thysanoessa* 属4種と異なり，北部北太平洋の浅海の沿岸水に区分される水塊にのみ出現し，*T. spinifera* は同じく *T. longipes*, *T. inermis* *T. inspinata* よりやや低鹹な沿岸水の影響を受ける海域にまで分布します。しかし太平洋の東側で，北はアラスカ海流にその分布が限られるため水温は他種に較べて高い値を示し，*T. longipes*, *T. inspinata* はより高温の外洋域に分布することが示されます。また，南極洋においては *E. superba* の北限域が明瞭に示され，この種の大量に分布する海域が南極収束線内の大陸側において，海域毎に局部的なかたよりがあることが示されました。

おきあみ類については，その摂餌行動，生殖行動と関連して，個体発生に伴なう鉛直行動を行なうことが示されます。海洋の深海系に分布する *Thysanopoda* 属のおきあみ類数種は，その Furcilia 期から未成熟期には浅海系下部から深海系上部に分布しますが，成体は深海系の中部から下部漸深海帯に分布し，摂餌，生殖行動を行ないます。おきあみ類はまたその成長段階において日周期鉛直移動の範囲が異なることも明らかにされました。

おきあみ類の生態的特性の中で，その摂餌構造と食性は興味ある課題の一つです。一般に第二次生産者として重要な *Euphausia* 属の各種は，浅海系で沪過捕食するのに適した胸脚および沪過刺

* 1978年6月29日，日仏会館(東京)にて講演
Résumé de la conférence faite le 29 juin 1978 après la remise du Prix de la Sociéte franco-japonaise d'océanogaphie

** 東京大学海洋研究所 Institut de Recherche Océanique, Université de Tokyo

毛をそなえるのが普通ですが，各節の長さの割合および各節に生える刺毛の長短，その間隔は，棲息する海域の餌料生物の分布状態と関連して種毎に異なる傾向が認められました。

南北両極の植物プランクトン現存量の多い海域の *Euphausia* 属の各種は，胸脚6対がそれぞれ発達し，沪過刺毛は5〜12 μ 程度の密な間隔で生えています。*Thysanoessa raschii* も同属の中で一種，高い植物プランクトン現存量を示す海域の浅海系で摂餌をする種類で，同じように8〜11 μ の密な間隔で刺毛が生えています。これに対して，より雑食性の性質を示す種では後部の胸脚が退行し，かつ沪過刺毛の間隔が大きく，刺毛の発達が弱くなることが示されます。*Euphausia* 属の最も有効な沪過節であると考えられる長節と基節の種間相対成長をみると2つの群に分かれ，*Euphausia* 属の中の沪過捕食種と亜熱帯域に分布する雑食性の *Euphausia* 属では異なる種間相対成長を示し，それぞれ現場の摂餌条件と対応した分化が認められます。

餌料の捕捉，破砕に用いられる大顎は，その摂餌特性と対応して臼歯部の発達する沪過捕食種と，切歯部の発達する肉食種とに分かれますが，海洋の鉛直分布と関連して，浅海系に分布する *Euphausia* 属のおきあみ類のうち両極海域に分布する種は臼歯部が発達し，熱帯域に分布する種はこの程度がやや弱くなる傾向が認められます。また胃内壁に生える刺毛は沪過捕食者において発達し，特に *E. superba* には刺環と呼ばれる破砕機構が胃後部に存在しますが，赤道海域付近に分布する *gibba* 群に属する *Euphausia* 属の各種はこの刺環が発達せず，むしろ切歯状のいくつかの刺により形成されています。

おきあみ類の捕食者としてはひげ鯨類が最も適応した一つの生物群であることは論を待ちません。ひげ鯨のうち私が研究した種は大型鯨を中心に10種類があげられます。そのうち，母船式捕鯨業，沿岸捕鯨業によって捕獲されていた種が6種類あり，また研究のために捕獲を許可されたセミクジラ *Eubalaena glacialis* が含まれていたことも幸運であったと申せましょう。

ひげ鯨類の摂餌についてはまずその摂餌構造を検討する必要があります。ひげ鯨の主な摂餌構造としては口角の形態，鯨ひげの形態，ひげ毛の性状，畝の有無，その延長の度合等が重要な形質となります。これらの形質の組合せにより，ひげ鯨類の摂餌型が三通りに分けられます。

一つは密な群集団をつくった動物プランクトン，マイクロネクトンを腹部下面の畝を利用して群ごと呑み込み，次に口腔内の両側に生えた鯨ひげによって水と餌を選り分けて胃に送る方法です。この型のひげ鯨としては，シロナガスクジラ *Balaenoptera musculus*，ナガスクジラ *B. physalus*，ザトウクジラ *Megaptera novae angliae* があります。これらの鯨は長距離にわたり，季節的に南北に大規模な回遊をする点を注目しなければなりません。極海域に回遊，または移動する生物のうち，鯨類についてはとくにこの点が強調されます。

次に，海洋にやや粗な分布を示す動物プランクトンを捕食する種があげられます。ひげ鯨の中ではセミクジラ *Eubalaena glacialis*，ホッキョククジラ *B. mysticetus* がこの群に属すると考えられます。セミクジラの餌は，過去の研究結果によれば，かいあし類を含む動物プランクトンが主要なものです。海の潮目に沿ってセミクジラの捕食活動を観察することも稀ではありません。セミクジラは1 m^3 当り数g程度分布するかいあし類，*Calanus plumchrus* や *C. finmarchicus* を捕食することも可能となります。また，この型のひげ鯨の回遊の規模は大きくないことが指摘されます。

捕食される動物プランクトン，マイクロネクトンの単位体積当りの個体数は，生物量の増大に伴ない減少します。大型の餌料種は単位体積当りの個体数が減少するわけですが，この極端な例としては *M. novae-angliae* に捕食されるスケトウダラやサバの群集団をあげることが出来ます。捕食者の摂餌条件より餌生物の生態的特性が明らかにされたことも注目すべき点の一つです。

この二つの型をとる鯨としてはイワシクジラ *B. borealis* があります。腹部下面の畝が他の *Balaenoptera* の種程延長せず，また鯨ひげの性状も

B. musculus 等の‘呑み込み型’のひげ鯨と *E. glacialis* の中間の性質を見せています。即ち，細いひげ毛を持つひげ板はやや長く沪過面積の増大を示し，上顎はやや弯曲してセミクジラと同じように連続しており，プランクトンを‘沪し取る’のに役立ちます。かつ畝を有効に使うことにより‘呑み込み型’の摂餌型をとることも可能です。

南極洋のイワシクジラは，かいあし類やおきあみ類の他に端脚類 *Parathemisto gaudichaudii* を捕食し，特に南極洋の低緯度においては主餌料となることが示されます。*P. gaudichaudii* はかいあし類を主に捕食するので，南極洋においては，

植物プランクトン──→おきあみ（*E. superba*）──→ひげ鯨

という最も短かい食物連鎖の他に，

植物プランクトン──→かいあし類──→端脚類（*P. gaudichaudii*）──→イワシクジラ（*B. borealis*）

の食物連鎖が存在することが明らかにされました。この食物連鎖は *E. superba* により形成される餌場と異なり，より広範囲の南大洋域に出現しますが，季節的にみてもより広い時期を摂餌場として形成すると考えられます。

イワシクジラは，南極洋への回遊の時期が他のシロナガスクジラやナガスクジラよりも遅れ，南極洋の言わば秋期に回遊が見られますが，これは端脚類による餌場の形成と結びつけられます。また，シロナガスクジラ，ナガスクジラ等，大型ひげ鯨類の減少に伴ない，イワシクジラの回遊の時期が早くなり，かつ摂餌行動圏がより南まで及ぶことが示された点も注目しなければなりません。

今後の研究課題においては引き続き大型動物プランクトン，マイクロネクトンの生態に関する研究が私にとって興味ある点となります。おきあみ類のみならず，あみ類，えび類，いか類，魚類等を含めて，生態系におけるこれらの生物群にわたる総合的な解析が重要と考えられます。特に海洋の深海系におけるマイクロネクトンの動態について研究を続けていきたいと考えます。

今回，日仏海洋学会賞を頂きましたことを機会に，これらの課題につきさらに努力を続けて参りたいと考えております。引き続き会員の皆様方の御指導をお願い申し上げます。

学　会　記　事

1. 昭和53年6月28日，東京水産大学において，編集委員会が開かれた。

2. 昭和53年6月23日，東京水産大学において評議員会が開かれた。
   1) 会務報告，編集報告が行なわれた。
   2) 昭和52年度の収支決算および昭和53年度の予算案が審議された。
   3) 学会賞候補者として根本敬久氏が推薦され，受賞者として決定した経過が報告された。
   4) 昭和53年度学会賞受賞候補者推薦委員15名を下記のとおり選出した。
   阿部友三郎，有賀祐勝，石野　誠，今村　豊，宇野寛，草下孝也，斎藤泰一，杉浦吉雄，高野健三，多賀信夫，根本敬久，星野通平，松生　洽，丸茂隆三森田良美

3. 昭和53年6月29日，日仏会館会議室において，第19回総会が開かれ，次の報告並びに審議が行われた。
   1) 昭和52年度の会務並びに会計報告が行われた。なお，別表の52年度収支決算が承認された。
   2) 編集委員長から学会誌第15巻の編集経過報告が行なわれた。第15巻は総ページ数217ページで，その内訳は原著論文14編（和文8，英文6），資料1編，記念講演1編，その他学会記事などである。
   3) 学会賞受賞者として根本敬久氏が決定に至る経過が報告された。
   4) 昭和53年度の予算案について審議の結果，別表のとおり承認された。
   5) 昭和53，54年度の評議員が選出された。（本誌169ページの評議員の名簿を参照）

昭和52年度収支決算

収　入

項　目	収入額(円)	備　考
前年度繰越金	22,630	
会　費	1,167,500	
賛助会費	425,000	
賛助費	20,000	
学会誌売上	108,150	
広告料	220,000	
計	1,963,280	

支　出

事　項	支出額(円)	備　考
学会誌等印刷費	1,720,400	
送料通信費	142,810	
編集費	3,150	
事務費	34,000	
交通費	15,640	
会議費	31,400	
次年度繰越金	15,880	
計	1,963,280	

昭和53年度予算案

収　入

事　項	収入額(円)	備　考
前年度繰越金	15,880	
会　費	1,200,000	
賛助会費	500,000	
学会誌売上	120,000	
広告料	250,000	
計	2,085,880	

支　出

事　項	支出額(円)	備　考
学会誌等印刷費	1,800,000	
送料通信費	150,000	
編集費	5,000	
事務費	40,000	
交通費	20,000	
会議費	40,000	
予備費	30,880	
計	2,085,880	

   6) 昭和53年度学会賞受賞候補者推薦委員の選出について報告があった。

4. 総会終了後，引続き学会賞の授与が行われた。
   昭和53年度学会賞受賞者: 根本敬久氏（東京大学海洋研究所），受賞課題: おきあみ類をめぐる生物生態に関する研究（別項「推薦理由書」参照）。会長か

ら根本博士に賞状，メダルおよび賞金が授与され，続いて受賞記念講演が行われた。

5. 講演終了後懇親会が開かれ盛会であった。

6. 昭和53年6月29日，30日の両日，日仏会館会議室において，昭和53年度「日仏海洋学会学術研究発表会」が次のとおり開かれた。

6月29日（木）

午前の部

1. 根室地震および人為的放水により誘起された牛込濠水の静振 …………°森谷誠生（気象協会），阿部友三郎（東理大・理）
2. 風による牛込濠水副振動について—縦および横方向の静振と副振動の減衰—…………………°矢内秋生（目白学園女子短大），阿部友三郎（東理大・理）
3. 濠水中ならびに沿岸に発生する Slick の解析—Moire の方法による Capillary Waves の解析—………………………… °高山晴光，川鍋　宏，阿部友三郎（東理大・理）
4. 水の濁りと魚の走流行動…°井上　実，有元貴文，大西睦夫（東水大）
5. 多要素流速計の較正実験と観測例 ………………………… 岡崎守良（理化学研究所）

午後の部

6. 石垣島川平湾の海藻植生と光合成活性 ……………………°大葉英雄，有賀祐勝（東水大）
7. 浜名湖の植物プランクトン…°村野正昭（東水大），千葉健治（東大・水産実験所）
8. フィコシアニンによる藍藻類生物量指標に関する研究…………………………………関　文威・°高原　豊（筑波大・生物科学系）
9. 中規模気圧変動による海洋長波の発生について ………………………… 冨永政英（鹿児島大・工）

第19回総会

学会賞授賞

学会賞受賞記念講演

オキアミ類をめぐる生物生態に関する研究 …………………………… 根本敬久（東大海洋研）

6月30日（金）

午前の部

10. 飛砂現象に関する研究—砂粒子の終端速度を推定する方法—………… °新井正一，内村竜二，原島近夫，阿部友三郎（東理大・理）
11. 海水の泡沫性に及ぼす海藻抽出物質の影響および泡沫層の水平方向の崩壊……… °森　幹樹，矢部信之，阿部友三郎（東理大・理）
12. 安定海水泡沫の飛散機構—16 mm Film による現場試料の解析—…… °小林　貴，桜井喜明，阿部友三郎（東理大・理）
13. ヨーロッパにおける栽培漁業，特にマグロ類の諸問題について…………… 宇野　寛（東水大）

午後の部

14. 新潟地方における漂泳漂着動物の組織学的観察 …………… 本間義治（新潟大・理，臨海実験所）
15. ナンキョクオキアミ大形成群体の移動について ………神田献二，°高木和徳，関　雄二（東水大）
16. 弧立島周縁の流れの場と温度場の乱れ—伊豆大島の場合について—…………石野　誠，大塚一志，磯打　勉，峰　雄二（東水大）
17. 黒潮冷水域の挙動と海山………………小長俊二，西山勝暢（気象研）

特別講演

海鷹丸のナンキョクオキアミ調査航海について（映画使用）…………………… 神田献二（東水大）

7. 新入会員（正会員）

氏　名	所　　属	紹介者
飯沢正人	東水大大学院生	宇野　寛
加藤重一	東水大　海洋環境工学科	松生　治
加納　敬	〃　　〃	〃
永沢祥子	東大　海洋研	丸茂隆三
沢本彰三	東海大　海洋学部	元田　茂
日清鉱業㈱開発室		
（賛助会員）		
㈱本地郷	代表取締役　宮本　悟	松生　治

退会者

正会員　松平康男，中野　旭，末広恭雄，浜上安司

逝　去　渡辺貫太郎

8. 会員の住所所属の変更

氏　名	新住所又は新所属
佐野　昭	神戸市生田区中山手通7-178 神戸海洋気象台
横平　弘	札幌市豊平区真栄200～63
杉森康弘	清水市折戸1000　東海大学海洋学部
松本　勝	高松市松島町2-14-11
青木三郎	北区赤羽台3-14-29

9. 交換及び寄贈図書

1)	研究実用化報告	27(3, 4, 5)
2)	函館海洋気象台，海上気象報告	第34号
3)	英国産業ニュース	5, 6, 7月号
4)	滋賀大学教育学部，湖沼実習施設論文集	No. 17
5)	海洋産業研究資料	9(2, 3, 4)
6)	航　海	第55号
7)	日本海区水産研究所，研究報告	第29号
8)	海洋時報	第9号
9)	農業土木試験場技報（D）水産土木	第20号
10)	宇佐臨海実験所，研究報告	24(1～2)
11)	広島日仏協会報	No. 67～70
12)	国立科学博物館研究報告A類(動物学)	4(2)
13)	横須賀市博物館研究報告(自然科学)	第24号
14)	横須賀博物館資料集	第1号
15)	鯨研通信	第315号
16)	釜山水産大学，海洋科学研究所，研究報告	第10巻
17)	水産試験研究機関，海洋観測資料	昭和48年度
18)	Science et Pêche	N° 273-275
19)	Publications Scientifiques et Techniques du Cnexo Catalogue au les Janvien	1978
20)	Ia gazette	N° 21, 22
21)	Annales Hydrographiques	5(747)
22)	Bulletin d'Information	N° 113
23)	American Museum Novitates	N° 2641
24)	CSK Newsletter,	No. 52
25)	Biology of The Commercial Fishes in The Inland Reservoirs of The North European Pare of The OSSR Territory	Vol. 32
25)	Mechanization and Automatization of Fishery Problems of Rational Exploitation of Fishes	Vol. 39
26)	Revue des Travaux de L'institut des Peches Maritimes	Vol. XIV

日仏海洋学会賞受賞候補者推薦理由書

氏　名:　根　本　敬　久　（東京大学海洋研究所）

題　名:　おきあみ類をめぐる生物生態に関する研究

推薦理由: おきあみは，海洋の動物プランクトンの中で量的に多く，またひげ鯨の餌料として，さらにそれ自身水産生物資源としての可能性を持ち，きわめて重要な生物群であると考えられる。根本敬久博士は，おきあみの分類，分布，食性について，さらにまたおきあみの主要な捕食者であるひげ鯨の食性，回遊等について，長年にわたり広範な研究を遂行し，おきあみを鍵種とする海洋生物の生態に関する幾多の重要な知見を明らかにした。

北太平洋，南極洋，インド洋をおおう広範な海域で得られた試料に基づいて，各海域におけるおきあみの水平・鉛直分布状態，摂餌器官，餌の種類，集群の構成，成長等について多角的な研究を行ない，高い評価を得た。すなわち，ベーリング海，北太洋，および南極洋における主要なおきあみの分布を明らかにし，新種1種を記載した。特に海表層で濃密な群れをつくるおきあみでは，胸脚，口器，消化管，特に胃が構造・機能上沪過捕食に適した機能を具えており，餌として植物プランクトンを大量に摂ることを明らかにした。

ひげ鯨の摂餌生態については，主に摂餌回遊，口部・畝の形態・性状，餌の種類と量，捕食行動，ひげ鯨間の餌をめぐる競合等の諸問題について貴重な成果を発表した。すなわち，ひげ鯨の摂餌型を呑み込み型，沪し取り型およびその複合型の三つに分けた。呑み込み型のひげ鯨の主な餌は濃密な群れをつくるおきあみであり，これは大規模な季節的摂餌回遊を行なう。一方，沪し取り型のひげ鯨はおきあみの他に，これより粗な群れをつくるかいあし類や端脚類，異尾類をも捕食，季節的摂餌回遊の範囲は狭いことを確かめた。南極洋においては，従来報告されていた植物プランクトン→おきあみ→ひげ鯨に至る食物連鎖系の他に植物プランクトン→かいあし類→端脚類→イワシクジラに至る鎖が存在することを発見し，南極洋の生態系について重要な知見を加えた。

根本博士はこれらおきあみをめぐる海洋生物生態の研究から，海洋生物の未利用資源の一つとして，南極洋，北太平洋のおきあみについて検討を進め，その資源的価値，資源開発を行なう際考慮すべき生物的特性，資源診断に必要なパラメーター等について，数多くの先駆的な論文を発表した。

以上述べたように，根本敬久博士はおきあみをめぐる海洋生物およびその資源に関してきわめて顕著な業績をあげた。本委員会はこれに対し同博士を本賞の受賞者として推薦する。

学会賞受賞候補者推薦委員会
委員長　草　下　孝　也

主　要　論　文

1959: Foods of baleen whales with reference to whale movements. Sci. Rep. Whales Res. Inst., **14**;

149-290.

1962: Food of baleen whales collected in recent Japanese Antarctic whaling expeditions. Sci. Rep. Whales Res. Inst., **16**; 89-103.

1967: Feeding pattern of euphausiids and differentiations in their body characters. Inform. Bull. Planktology Japan Comm. Dr. Y. Matsue's 60th Birthday Anniv. vol., 157-171.

1968: Feeding of baleen whales and krill, and the value of krill as a marine resource in the Antarctic. Ant. Oceanography, 241-250.

1969: Euphausiaces dans les couches intermediaire et profonde. La mer, **7**; 50-55.

1972: Chlorophyll pigments in the stomach and gut of some macrozooplankton. Biological Oceanography of the North Pacific Ocean, 411-418.

1975: Present status of exploitation and biology of krill in the Antarctic. Oceanology International **75**; 353-360.

1977: Food and feeding structures of deep sea *Thysanopoda* euphausiids. Proceeding of International symposium on Sound Scattering In the Sea. Oceanic Sound Scattering Prediction, 457-480.

1977: Characteristics of food habits and distribution of baleen whales with special reference of the abundance of North Pacific Sei/Bryde's whales. (In the press, Papers in Sei whales Conference, Whaling Commission Supplement).

お　知　ら　せ

FGGE 期間中の海洋調査計画の報告について

FGGE (First GARP Global Experiment: 1978年12月1日～1979年11月30日) 期間中に予定されている海洋調査計画の報告について，多くの海洋学研究者が，IOC (政府間海洋学委員会) 事務局長からの依頼文書および同封された「Projected Observational Plans Form」の記入用紙を受け取られたと思います。

依頼文にも書いてあるように，本来はこの種の事務は国際海洋資料交換 (IODE) 組織を通じて行われるべきものでありますが，既に FGGE 期間に入っており時間的余裕がないため，取り急ぎ直接研究者個人宛に依頼されたものであります。ここに国際海洋資料交換国内調整員の立場から本件への御協力をお願するとともに，本件に関するガイドを述べたいと思います。

IOC の依頼文書の主旨は次のとおりです。

FGGE 期間中に予定されている海洋調査計画を同封のフォームに記入し，米国の NOAA にある RNODC-FOY (FGGE 実施年の責任国立海洋資料センター) へ早急に送付されたい。これは RNODC-FOY に課せられた次の二つの業務

(1)「全地球的海洋学データ目録」の作成

(2)「全地球的海洋気候データベース」の作成

の中の前者のためのものである。

本目録は，FGGE 期間中に観測された総ての海洋学データ (生物，化学，物理，地質) の案内役を果すものである。RNODC-FOY は記入された「Projected Observational Plans Form」から本目録を編集公刊する。その初版は1979年6月と予定されている。なおこの目録は観測終了後に観測データ項目等の明細を示す「海洋調査報告 (ROSCOP) の送付によってチェックされることになっている。

「全地球的海洋気候データベース」は，FGGE 期間中に観測されたすべての利用可能データ (塩分，水温，海流，海面水位，燐酸塩，珪酸塩，溶存酸素) により作成される。これらのデータ交換は「国際海洋資料交換の手引き」に従って国際海洋交換チャネルを通じて実施される。即ち観測終了後2年以内に，国内の海洋資料センターでの標準化処理を経て RNODC-FOY に送付される。RNODC-FOY は更に2年以内に全データベース作成を完了して世界資料センター(海洋学)へ送付し一般利用者の便に供する。

FGGE を成功させる為には，これら海洋データ目録とデータの提供に関しての貴方の協力いかんにかかっている。

以上が依頼の主旨ですが，本件に関連して二，三の要望を述べます。

1. 「Projected Observational Plans Form」の送付方法

（下記 (a), (b) いずれの方法でも結構です。）

(a) 海洋資料センター経由

必要事項記入後，海洋資料センターへ送付されたい。センター記入事項チェックの上，一括して RNODC-FOY へ送付します。

(b) RNODC-FOY へ直送

直接 RNODC-FOY へ既に送付されたものまたは今後送付予定のものは，今後のフォローのために，そのコピーを海洋資料センターに送付されたい。宛名はフォームに明示されている。

2. 記入フォームの記載内容について次の事項が不明確なので RNODC-FOY へ照会したところ，記入フォーム 5), 6) の Processing Center は，普通は第一次処理を行う調査機関を，12) の Residence of final data は普通は海洋資料センターを記入するとのことです。従って 12) は下記のように記入して下さい。

JAPAN OCEANOGRAPHIC DATA CENTER
Hydrographic Department, Maritime Safty Agency
No. 3-1, Tsukiji 5-chome, Chuo-ku, Tokyo, 104
JAPAN　(PHONE 03-541-3811)

3. 記入フォームへの登録基準については，毎年海洋資料センターへ提出されている国内海洋調査計画の中の DNP（宣言された国内計画）は当然この登録に含まれますが，更に以外のクルーズについても可能な限り登録されるよう希望します。

また昭和54年4月以降の調査計画がまだ不確定の場合はとりあえず3月までのものを報告し，4月以降の分は確定次第報告するようにした方がよいと思います。

4. 今後の業務について

今回登録されるクルーズの海洋調査報告(ROSCOP)は，観測終了後なるべく速かに，また該当するデータは観測終了後おそくとも2年以内，出来れば1年半以内に海洋資料センター宛送付をお願い致します。

5. その他

IOC の依頼文書が個人宛になっているため，或る機関の一調査航海について重複して RNODC-FOY へ送付されるおそれがありますが，海洋資料センターへ送付される場合は同センターで調整しますが，直接 RNODC-FOY へ送付される場合は，機関内に重複をさけるための調整がなされるよう希望します。

記入用紙が不足の場合は，コピーしていただくか当センターへ請求して下さい。

海洋資料センター（国際海洋資料交換国内調整員）
二　谷　穎　男記

日仏海洋学会役員

顧　問　ユベール・ブロッシェ　ジャン・デルサルト　ジャック・ロベール　アレクシス・ドランデール　ベルナール・フランク

名誉会長　ミシェル・ルサージェ

会　長　佐々木忠義

副会長　黒木敏郎，國司秀明

常任幹事　阿部友三郎，宇野　寛，永田　正

庶務幹事　三浦昭雄

編集幹事　有賀祐勝

幹　事　石野　誠，井上　実，今村　豊，岩下光男，川原田　裕，神田献二，菊地真一，草下孝也，斎藤泰一，佐々木幸康，杉浦吉雄，高木和徳，高野健三，辻田時美，奈須敬二，根本敬久，半沢正男，松生　洽，丸茂隆三，森田良美，山中鷹之助　（五十音順）

監　事　久保田　穣，岩崎秀人

評議員　青山恒雄，赤松秀雄，秋山　勉，阿部宗明，阿部友三郎，新崎盛敏，有賀祐勝，石野　誠，石渡直典，市村俊英，井上　実，今村　豊，入江春彦，岩崎秀人，岩下光男，岩田憲幸，宇田道隆，宇野　寛，大内正夫，小倉通男，大村秀雄，岡部史郎，岡見　登，梶浦欣二郎，加藤重一，加納　敬，川合英夫，川上太左英，川村輝良，川原田　裕，神田献二，菊地真一，草下孝也，楠　宏，国司秀明，久保田　穣，黒木敏郎，小泉政美，小林　博，小牧勇蔵，西条八束，斎藤泰一，斎藤行正，佐伯和昭，坂本市太郎，佐々木忠義，佐々木幸康，猿橋勝子，椎野季雄，柴田恵司，下村敏正，庄司大太郎，杉浦吉雄，関　文威，多賀信夫，高木和徳，高野健三，高橋淳雄，高橋　正，谷口　旭，田畑忠司，田村　保，千葉卓夫，辻田時美，寺本俊彦，鳥羽良明，富永政英，鳥居鉄也，中井甚二郎，中野猿人，永田　正，永田　豊，奈須敬二，奈須紀幸，西沢　敏，新田忠雄，根本敬久，野村　正，半沢正男，半谷高久，樋口明生，菱田耕造，日々谷　京，平野敏行，深沢文雄，深瀬　茂，福島久雄，淵　秀隆，星野通平，増沢穣太郎，増田辰良，松生　洽，松崎卓一，丸茂隆三，三浦昭雄，三宅泰雄，宮崎千博，宮崎正衛，村野正昭，元田　茂，森川吉郎，森田良美，森安茂雄，安井　正，柳川三郎，山路　勇，山中鷹之助，山中一郎，山中　一，吉田多摩夫，渡辺精一　（五十音順）

マルセル・ジュグラリス，ジャン・アンクティル，ロジェ・ペリカ

賛　助　会　員

旭化成工業株式会社	東京都千代田区有楽町 1-1-2　三井ビル
株式会社内田老鶴圃新社　内田悟	東京都千代田区九段北 1-2-1　蜂谷ビル
大金久展	東京都港区新橋 3-1-10　丸藤ビル　社団法人　海洋産業研究会
株式会社　オーシャン・エージ社	東京都千代田区神田美土代町 11-2　第1東英ビル
株式会社大林組	東京都千代田区神田司町 2-3
小樽船用電機株式会社	小樽市色内町 3-4-3
株式会社オルガノ	東京都文京区本郷 5-5-16
株式会社　海洋開発センター	東京都港区赤坂 1-9-1
協同低温工業株式会社	東京都千代田区神田佐久間町 1-21　山伝ビル
協和商工株式会社	東京都豊島区目白 4-24-1
小松川化工機株式会社	東京都江戸川区松島 1-342
小山康三	東京都文京区本駒込 6-15-10　英和印刷社
三信船舶電具株式会社	東京都千代田区神田 1-16-8
三洋水路測量株式会社	東京都港区新橋 5-23-7　三栄ビル
シュナイダー財団極東駐在事務所	東京都港区南青山 2-2-8　DF ビル
昭和電装株式会社	高松市寺井町 1079
新日本気象海洋株式会社	東京都渋谷区東 1-19-3　青山ビル
株式会社鶴見精機	横浜市鶴見区鶴見町 1506
東亜建設工業株式会社	東京都千代田区四番町 5
東京工材株式会社	東京都中央区築地 4-7-1　築三ビル
株式会社東京久栄	東京都中央区日本橋 3-1-15　久栄ビル
東京製綱繊維ロープ株式会社	東京都中央区日本橋室町 2-6　江戸ビル
株式会社東邦電探	東京都杉並区宮前 1-8-9
中川防蝕工業株式会社	東京都千代田区神田鍛冶町 2-2-2　東京建物ビル
株式会社ナック	東京都港区西麻布 1-2-7　第17興和ビル
日本アクアラング株式会社	東京都杉並区方南町 2-4-7　第2細野ビル
日本海洋産業株式会社	東京都新宿区西新宿 2-6-1　新宿住友ビル
日本テトラポッド株式会社	東京都港区新橋 2-1-13　新橋富士ビル9階
社団法人　日本能率協会	東京都港区芝公園 3-1-22　協立ビル
日本プレスコンクリート株式会社	東京都中央区日本橋本石町 1-4
深田サルベージ株式会社	東京都千代田区神田錦町 1-9-1　天理教ビル8階
藤田潔	東京都新宿区四谷 3-9　光明堂ビル　株式会社ビデオプロモーション
藤田峯雄	東京都江東区南砂 1-3-25　株式会社 中村鉄工所
フランス物産株式会社	東京都千代田区神田小川町 3-20-2　増淵ビル
古野電気株式会社	東京都中央区八重洲 4-5　藤和ビル
丸文株式会社	東京都中央区日本橋大伝馬町 2-1-1
三井海洋開発株式会社	東京都千代田区霞ケ関 3-2-5　霞ケ関ビル 3002号室
吉野計器製作所	東京都北区西ケ原 1-14
株式会社離合社	東京都千代田区神田鍛冶町 1-10-4
株式会社渡部計器製作所	東京都文京区向丘 1-7-17

昭和 53 年 8 月 25 日 印刷
昭和 53 年 8 月 28 日 発行　　うみ　　第 16 巻 第 3 号

定価 ¥950

編集者　冨永政英
発行者　佐々木忠義
発行所　日仏海洋学会
財団法人 日仏会館内
東京都千代田区神田駿河台2-3
郵便番号：101
電話：03(291)1141
振替番号：東京96503

印刷者　小山康三
印刷所　英和印刷社
東京都文京区本駒込 6-15-10
郵便番号：113
電話：03(941)6500

第 16 巻　第 3 号

目　次

Tome 16　N° 3

SOMMAIRE